UNIVERSIDAD AUTÓNOMA DE SAN LUIS POTOSÍ

FACULTAD DE CIENCIAS QUÍMICAS

PROGRAMA DE POSGRADO EN BIOPROCESOS

EFECTO DE LAS NANOPARTÍCULAS DE PLATA EN EL SISTEMA NERVIOSO CENTRAL

TESIS QUE PARA OBTENER EL GRADO DE

DOCTOR EN CIENCIAS EN BIOPROCESOS

PRESENTA:

M.C. SAMUEL SALAZAR GARCÍA

DIRECTOR DE TESIS:
DRA. MARÍA DEL CARMEN GONZÁLEZ CASTILLO

SAN LUIS POTOSÍ, S. L. P. SEPTIEMBRE DE 2020

UNIVERSIDAD AUTÓNOMA DE SAN LUIS POTOSÍ

FACULTAD DE CIENCIAS QUÍMICAS

PROGRAMA DE POSGRADO EN BIOPROCESOS

EFECTO DE LAS NANOPARTÍCULAS DE PLATA EN EL SISTEMA NERVIOSO CENTRAL

TESIS QUE PARA OBTENER EL GRADO DE

DOCTOR EN CIENCIAS EN BIOPROCESOS

PRESENTA:

M.C. SAMUEL SALAZAR GARCÍA

DIRECTOR DE TESIS:
DRA. MARÍA DEL CARMEN GONZÁLEZ CASTILLO

SINODALES

PRESIDENTE:
DRA. MARÍA DEL CARMEN GONZÁLEZ CASTILLO _____
SECRETARIO:
DR. SERGIO ROSALES MENDOZA _____
VOCAL:
DRA. CLAUDIA CASTILLO MARTÍN DEL CAMPO _____
VOCAL:
DR. GABRIEL ALEJANDRO MARTÍNEZ CASTAÑÓN _____
VOCAL:
DR. ABEL SANTAMARÍA DEL ÁNGEL _____

SAN LUIS POTOSÍ, S. L. P. SEPTIEMBRE DE 2020

Proyecto realizado en:

Laboratorio de Fisiología Celular de la Facultad de Ciencias Químicas, Universidad Autónoma de San Luis Potosí.

Con financiamiento de: Beca-Tesis del Consejo Nacional de Ciencia y Tecnología (CONACYT): 278347.

"El programa de Maestría o Doctorado en Ciencias en Bioprocesos de la Universidad Autónoma de San Luis Potosí Pertenece al Programa Nacional de Posgrados de Calidad (PNPC) del CONACyT, registro 000588 (Maestría) 000590 (Doctorado), en el Nivel Maestría (Consolidado) Doctorado (En Desarrollo). Número de registro de becario CONACyT: 278347.

Agradecimientos académicos

A mi asesora, Dra. María del Carmen González Castillo por abrir las puertas de su laboratorio y grupo de investigación, permitiéndome una formación de gran calidad académica y humana, no solo en el doctorado, sino también en la maestría y la licenciatura.

Al Dr. Juan Manuel Vargas Morales y su grupo de trabajo en el Laboratorio de Análisis Clínicos de esta universidad, por toda su asesoría y apoyo técnico y humano.

Al Dr. Gabriel Alejandro Martínez Castañón por su colaboración en la síntesis y caracterización de las nanopartículas de plata.

A la Dra. Claudia Castillo Martín del Campo por su asesoría y apoyo en la obtención de cortes histológicos.

Al Dr. Abel Santamaria del Ángel y su grupo de trabajo del Laboratorio de Aminoácidos Excitadores del Instituto Nacional de Neurología y Neurocirugía, por toda su asesoría científica.

A la Dra. Norma Laura Delgado Buenrostro y todo el equipo de trabajo del Laboratorio de Toxicología y Carcinogénesis de la Facultad de Estudios Superiores Iztacala, Universidad Nacional Autónoma de México, por todo su apoyo técnico y científico en la obtención de imágenes histológicas.

A la Dra. Diana Patricia Portales Pérez por su asesoría y apoyo en la citometría de flujo.

A toda la comunidad que conforma la Facultad de Ciencias Químicas y el Centro de Investigación en Ciencias de la Salud y Biomedicina de la UASLP.

Agradecimientos personales

A mis compañeros del Laboratorio de Fisiología Celular: Sonia, Lily, Blanca, Norma, Denisse, Jimena, Pedro Pablo, Diego, Héctor, Alex, Memo, Paco, José, Rafa, Capu, por todo el trabajo en equipo y las horas que convivimos dentro de nuestras actividades en el laboratorio. Un agradecimiento muy grande hasta el cielo a ti amigo Daniel.

A todos mis estudiantes de las diferentes instituciones donde he tenido la dicha de ser su profesor. Dice una frase célebre que enseñar es la mejor forma de aprender.

A todos ustedes: Claudia, Mary Ángeles, Jaime y Oswaldo. Su apoyo y motivación constante me han ayudado mucho en la culminación de este proyecto de vida.

A mi familia: Mi mamá, mi papá hasta el cielo, mis hermanas Rita y Gaby, mis sobrinos Santi y Elenita, mis tías Ester y Juani, mis abuelitos hasta el cielo y al resto de primos y tíos. Ustedes han sido un soporte constante en este y todos mis proyectos de vida. Contar con todos ustedes ha sido una gran bendición.

Finalmente agradezco a Dios por permitirme estudiar parte de su maravillosa existencia a través de la ciencia.

Contenido

Capítulo 1

Zinc protects the rat brain from damage induced by 24 h exposure to silver nanoparticles

Resumen en inglés

Silver nanoparticles (AgNPs) have been widely employed due to their antimicrobial properties; however, several studies sustain that AgNPs can induce brain damage, like the blood–brain barrier (BBB) disruption. Among the BBB defense mechanisms, the metallothioneins (MTs), a collection of proteins that regulate intracellular levels of zinc (Zn), play an important role. The goal of this work was to investigate whether the brain damage caused by an intraperitoneal administration of AgNPs (15 mg/g body weight) at the level of the BBB permeability disruption, damage of the brain tissue, and systemic inflammation could be prevented by 24 h of previous treatment with Zn (27 mg/kg body weight). Evans blue (EB) extravasation, modification of claudin-5 expression, alterations on MTs, N-cadherin expression, and systemic inflammation were evaluated. Our results show that AgNPs induce BBB damage by increasing EB extravasation and decreasing claudin-5 expression, associated with overexpression of MTs, effects that were related with systemic inflammation, evidenced by the increase of granulocytes. Zn pretreatment partially prevented the BBB permeability from the damage induced by AgNPs, whereas the MTs expression and granulocytes count exhibited a reversal effect, suggesting that the effect of Zn could be related with the BBB regulation process. The rat brain histological analysis confirmed that pretreatment with Zn prevented at least in part the toxic effect of AgNPs. This work provides relevant information about the role of Zn as a protectant against the noxious effects of AgNPs upon the rat brain physiology.

Keywords: Silver nanoparticles; Brain; Blood Brain Barrier; Metallothioneins; Zinc; Protection.

Resumen en español

Las nanopartículas de plata (AgNPs) se han empleado por sus propiedades antimicrobianas. Sin embargo, varios estudios sostienen que las AgNPs pueden inducir daño cerebral, por ejemplo una disfunción de la barrera hematoencefálica (BHA). Entre los mecanismos de defensa de la BHA se encuentran las metalotioneínas (MTs), un grupo de proteínas que juegan un papel importante en la regulación de los niveles intracelulares de zinc (Zn). El objetivo de este trabajo consistió en investigar si una administración intraperitoneal de AgNPs (15 mg / g peso corporal) causaba daño a nivel de la permeabilidad de la BHA, tejido cerebral e inflamación sistémica, y si este daño pudiera prevenirse con 24 h de tratamiento previo con Zn (27 mg/ kg de peso corporal). La extravasación de azul de Evans (EB), la expresión de claudina-5, MTs, y N-cadherina e inflamación sistémica fueron evaluados. Nuestros resultados muestran que las AgNPs inducen daño en la BHA, aumentando la extravasación de EB y disminuyendo la expresión de claudina-5, efectos asociados con una sobreexpresión de MTs, efectos que a su vez estaban relacionados con una inflamación sistémica, evidenciado por el aumento de granulocitos. El pretratamiento de Zn impidió parcialmente el daño en la BHA inducido por las AgNPs, mientras que la expresión de MTs y el recuento de granulocitos exhibió un efecto de reversión, lo que sugiere que el Zn podría estar regulando el daño a nivel de BHA. El análisis histológico de cerebro de rata confirmó que el pretratamiento con Zn previno, al menos en parte el efecto tóxico de las AgNPs. Este trabajo proporciona información relevante sobre el papel del Zn como protector contra los efectos nocivos de las AgNPs en la fisiología del cerebro de la rata.

Palabras clave: Nanopartículas de plata, Cerebro, Barrera Hematoencefálica, Zinc, Protección.

Zinc protects the rat brain from damage induced by 24 hours exposure to silver nanoparticles

Samuel Salazar-García[a, b], Norma Laura Delgado-Buenrostro[c], Juan Carlos Rodríguez Escamilla[c], Guillermo Davalos-Rivas[a,b], Yolanda Irasema Chirino[c], Claudia G. Castillo Martín del Campo[d], Gabriel A. Martínez-Castañón[e], Juan Manuel Vargas-Morales[a], Carmen Gonzalez[a,b]

[a]Universidad Autonoma de San Luis Potosi, Facultad de Ciencias Quimicas, San Luis Potosí, Mexico.

[b]Universidad Autonoma de San Luis Potosi, Centro de Investigación en Ciencias de la Salud y Biomedicina, San Luis Potosi, Mexico.

[c]Universidad Nacional Autonoma de Mexico, Unidad de Biomedicina, Facultad de Estudios Superiores Iztacala, Estado de Mexico, Mexico.

[d]Universidad Autonoma de San Luis Potosi, Facultad de Medicina, San Luis Potosi, Mexico.

[e]Universidad Autónoma de San Luis Potosi, Facultad de Estomatologia, San Luis Potosi, Mexico.

Corresponding author: Carmen Gonzalez, Ph. D.

Address: Facultad de Ciencias Quimicas, Universidad Autonoma de San Luis Potosi, Av. Manuel Nava No. 6., Col. Universitaria. Zip Code 78210, San Luis Potosi, Mexico.

Phone: +52-444-8262440 x 6459; **E-mail:** gonzalez.castillocarmen@uaslp.mx**;** cgonzalez.uaslp@gmail.com

1. Abstract

Silver nanoparticles (AgNPs) have been widely employed due to their antimicrobial properties; however, several studies sustain that AgNPs can induce brain damage, like the the blood brain barrier (BBB) disruption. Among the BBB defense mechanisms, the metallothioneins (MTs), a collection of proteins that regulate intracellular levels of zinc (Zn) play an important role. The goal of this work was to investigate whether the brain damage caused by an intraperitoneal administration of AgNPs (15 mg / kg body weight) at the level of the BBB permeability disruption, damage of the brain tissue and systemic inflammation could be prevented by 24 hours of previous treatment with Zn (27 mg / kg body weight). Evans blue (EB) extravasation, modification of claudin-5 expression, alterations on MTs, N-cadherin expression and systemic inflammation were evaluated. Our results show that AgNPs induce BBB damage by increasing EB extravasation and decreasing claudin-5 expression, associated with overexpression of MTs, effects that were related with systemic inflammation, evidenced by the increase of granulocytes. Zn pretreatment partially prevented the BBB permeability from the damage induced by AgNPs, whereas the MTs expression and granulocytes count exhibited a reversal effect, suggesting that the effect of Zn could be related with the BBB regulation process. The rat brain histological analysis confirmed that pretreatment with Zn prevented at least in part the toxic effect of AgNPs. This work provides relevant information about the role of Zn as a protectant against the noxious effects of AgNPs upon the rat brain physiology.

Keywords: Silver nanoparticles; Brain; Blood Brain Barrier; Metallothioneins; Zinc; Protection.

Abbreviations: BCA, bicinchoninic acid; BBB, Blood Brain Barrier; CNS, Central nervous system; DLS, Dynamic light scattering; EB, Evans Blue; IC. Intracarotid; ICV, Intracerebroventricular; IP, Intraperitoneal; IV, Intravenous; GAPDH, Glyceraldehyde-3-phosphate dehydrogenase; GRA, Granulocytes; LY, Lymphocytes; MTs, Metallothioneins; MID, Monocytes; DMF, N,N-Dimethylformamide; NMs, Nanomaterials; PLT, Platelets; RBC, Red blood cells; AgNPs, Silver nanoparticles; $AgNO_3$, Silver nitrate; TJ, Tight junctions; TEM, Transmission electron microscopy; WBC, White blood cells; Zn, Zinc; $ZnCl_2$, Zinc Chloride.

2. Introduction

Nanotechnology is defined as a discipline dedicated to the study and development of systems at nanometer scale (1-100 nm), named nanomaterials (NMs), (British Standards Institution 2007; Liu et al. 2013). Silver nanoparticles (AgNPs) are NMs with quite a lot of applications mostly due to their antimicrobial properties. Among the application areas of AgNPs are optical, electrical and biological, which are constantly increased and incorporated into society through a wide range of products (Chen and Schluesener 2008; Gonzalez et al. 2016). It is estimated that about 30% of nanotechnology based consumer products contain AgNPs (Liu et al. 2017). However, it has also been addressed that AgNPs possess a wide diversity of biological effects (AshaRani et al. 2009) which vary depending on the NPs size, shape, concentration, cellular target and exposure route (Gliga et al. 2014; Rosas-Hernandez et al. 2015), all of them being parameters that could confer beneficial, protective or harmful effects to living organisms.

The AgNPs can be distributed to the whole organism through the cardiovascular system (Oberdörster et al. 2005), eventually reaching the central nervous system (CNS). In this system, neurons, together with highly specialized cerebral capillaries and pericytes, constitute the Blood Brain Barrier (BBB), defined as the frontier that separates the brain tissue from the circulating substances in the vascular system (Zlokovic 2008; Luther et al. 2011). The BBB function is to regulate the permeability through the exchange of substances from the blood to the brain and *vice versa*; this process is mediated by a protein complex, named tight junctions (TJ) located between the BBB capillary endothelial cells. TJ are

formed by a series of integral proteins located on the capillary endothelial cell membrane like claudin-5, occludine and adhesion molecules associated to cytoplasmic proteins like ZO1, linked to actin (Wen et al. 2014). The molecules responsible for the induction and maintenance of BBB properties are poorly known; however, several studies suggest that N-cadherin (transmembrane glycoproteins which mediate cell–cell contact in a calcium-dependent manner) expression by brain cells represents an initial and transient signal, which may be involved in the commitment of blood vessels to regulate BBB properties (Gerhardt 1999). Hence, despite the BBB operates as an effective defense mechanism of the CNS (Tsukita and Furuse 1999), several exogenous and endogenous factors or conditions could compromise its functionality and consequently, the brain integrity. For instance, the systemic inflammation characterized by the alteration of blood cell components like granulocytes is caused by several agents that in turn increase the permeability of the microvasculature and promotes the release of blood components into the extravascular tissues (Huber et al. 2001).

Several studies have shown that AgNPs can compromise the BBB functionality, depending on the particle size, dose and route of administration. In this regard, it is known that smaller nanoparticles (<10 nm) tend to be more toxic (Sharma and Ali 2006; Sharma et al. 2009a; Trickler et al. 2010). If BBB integrity is eventually compromised, the body may use alternative and adaptive mechanisms in order to restore the damage or protect against its development and progression. Zinc (Zn) is an essential metal responsible for several endogenous functions, that *per se* has been described as an antioxidant and anti-inflammatory agent (Kim et al. 2015). The protective effects of Zn are also associated with the metallothioneins (MTs) expression (Ruttkay-Nedecky et al. 2013), which are a series of low molecular weight proteins enriched with cysteine residues (Ioachim et al. 2000; Coyle et al.

2002), playing an important role as antioxidant, detoxifying heavy metals, due to the ability of cysteine residues to sequestrate metal ions and oxygen free radicals in a large number of cell types, including brain cells (Luther et al. 2011, 2012).

To date, there are multiple and controversial scientific evidences related to the AgNPs brain toxicity, most of them upon the BBB alteration (Sharma et al. 2009 a, b; Trickler et al. 2010); however, few studies related to the repair or reversion mechanisms associated to toxicity promoted by AgNPs are reported. In this context, we decided to evaluate the possible protective role of Zn on the brain damage induced by AgNPs, using as source of Zn, the $ZnCl_2$ as referred by other authors (Franciscato et al. 2011; Baiomy et al. 2015). We evaluated whether the pre-administration of Zn could exert a protective effect against the deleterious actions induced by AgNPs on BBB permeability, alteration of the MTs and N-cadherin expression, damage of the brain tissue and their association to the systemic inflammation.

Considering this background, the aim of this work was to investigate whether the damage induced by AgNPs (< 10 nm) upon the brain physiology and integrity, is prevented by a Zn pretreatment.

3. Methods

3.1 Chemicals

Evans Blue (EB) dye, zinc chloride ($ZnCl_2$), horseradish peroxidase (HRP)-secondary antibody, impregnation with silver nitrate and other chemical reagents were purchased from Sigma Aldrich Inc. (St. Louis, MO). $AgNO_3$ and N, N-Dimethylformamide (DMF) was purchased from Fermont Laboratories (Monterrey, Mexico), eosin was purchased from Hycel

Reactivos Quimicos (Zapopan, Mexico), saline solution was obtained from Pisa laboratories (Guadalajara, Mexico), antibodies against claudin-5 were acquired from Abcam (Cambridge, MA), MTs antibodies were obtained from Santa Cruz Biotechnology, and anti-CD325 (N-cadherin) antibody was obtained from Biolegend (San Diego, CA.).

3.2 Synthesis of AgNPs

AgNPs were synthesized previously described by (Espinosa-Cristobal et al. 2013). AgNPs with spherical shape were synthesized from a 0.35 M $AgNO_3$ solution placed in a 250 mL reaction vessel. Under magnetic stirring, 10 mL of deionized water containing gallic acid (0.1 g) was added to 100 mL of Ag^+ solution. After the addition of gallic acid, the pH of the solution was immediately adjusted to 11 with 1.0 M NaOH. Afterwards, the solution was heated for 30 min at 80 °C, and the final concentration of AgNPs used for *in vivo* treatments was 3,500 µg/mL.

3.3 AgNPs characterization

AgNPs were characterized using a dynamic light scattering (DLS) assay to determine hydrodynamic particle size, using a DLS Malvern Zetasizer Nano ZS (Instruments Worcestershire, United Kingdom), operating with a He-Ne laser at a wavelength of 633 nm, and a detection angle of 90°. All samples were analyzed for 60 s at 25 °C. To confirm shape and particle size, each sample was diluted with deionized water, and 50 µL of each suspension was placed on a copper grid for transmission electron microscopy (TEM); the AgNPs size by this technique was calculated with the average of 400 particles, using the ImageJ software. All samples were analyzed using a JEOL JEM-1230 microscope at an accelerating voltage of 100 kV.

3.4 Animals and treatments

To evaluate the effect of AgNPs on brain damage, adult male Wistar rats (250-300g) were divided into 4 groups (n=11 animals per group). The first group received an intraperitoneal (IP) administration of saline solution; the second group (as Zn exposure control) received an IP dose of $ZnCl_2$ (27 mg/kg body weight, accordingly to (Franciscato et al. 2011); the third group (damage control by AgNPs) received an IP dose of AgNPs (15 mg/kg body weight) for 24 hours; and to evaluate the possible protective role of zinc, the fourth group received an IP dose of $ZnCl_2$ (27 mg/kg body weight) and 24 hours later an IP dose of AgNPs (15 mg/kg body weight). From each group 8 animals were employed to evaluate the BBB permeability and the protein expression by western blot.

In addition, 3 animals per group were destined for the histological and blood components analysis**.** All experiments were performed in accordance with the National Institutes of Health guide for care and use of laboratory animals, and approved by the Animal Care and Use Committee of the Faculty of Chemistry of the University of San Luis Potosi (CEID2017109R1).

3.5 Evans blue extravasation

In order to analyze the BBB disruption, the Evans blue (EB) technique was used following the method by (Sharma and Ali 2006). After the animals were anesthetized and the blood samples were collected, a solution of EB dye (45 mg/kg) was injected into the jugular vein and allowed to circulate in the bloodstream for 2 hours. Later on, the animals were euthanized and transcardially perfused with 150 mL of phosphate buffer solution (PBS) pH 3.0. The brains were removed and separated into right and left hemispheres to minimize the number of animals used, since there was no difference in the appearance between the two hemispheres. The right hemisphere was immersed in 1 mL DMF and incubated for 18 hours at 80 ˚C, and then centrifuged (13,200 rpm, 1 hour, 4 ˚C); the supernatant was collected and

the absorbance was measured at 620 nm. Values were interpolated in a standard curve of EB in DMF, and data were expressed as µg of EB/g of brain tissue.

3.6 Western blot analysis

Modifications in claudin-5 and MTs protein expression were analyzed using the left hemisphere of each rat brain. Hemisphere samples were collected and homogenized in a radioimmunoprecipitation buffer, and the protein concentration was determined by the bicinchoninic acid (BCA) method. 50 µg of protein sample were loaded into sodium dodecyl sulfate-polyacrylamide gels, then run for 60 minutes at 200 mV and transferred into polyvinylidene fluoride membranes for 30 minutes at 100 mV. Membranes were blocked with 5% bovine serum albumin and then incubated overnight at 4 ˚C in primary antibody (1:200). Membranes were washed and incubated with secondary antibody (1:5000) during 2 hours and revealed with an HRP kit. Images were digitalized and analyzed using ImageJ software, and normalized to glyceraldehyde 3-phosphate dehydrogenase (GAPDH).

3.7 Brain histology

An additional group of male Wistar rat (250-300g) (n = 3) were used for the histological analysis. After treated, the animals were sacrificed by an overdose injection of sodium pentobarbital and the brain tissue immediately were prefixed by cardiac perfusion using 10% paraformaldehyde, and subsequently preserved in 30% sucrose. Tissue samples were dehydrated graded ethanol, embedded in paraffin and cut at 3-µm thickness. For histological examination, cortex sections were stained with the alkaline acid contrast technique hematoxylin-eosin, the silver impregnation technique Cajal and differential interference contrast (Nomarski). The images were obtained in a Leica TCS SP8 inverted confocal laser-scanning microscope.

3.8 Immunohistochemistry for N-cadherin

The paraffin-embedded sections of brain ($n = 3$) were analyzed for the presence of N-cadherin by Immunohistochemistry, according to Soler et al. (1997). Paraffin sections were dewaxed, rehydrated and blocked with 1% BSA. Then, cells were permeated in 1% PBS-triton X100 for 7 min at 27 °C, and washed with PBS. Sections were incubated overnight at 4°C with mouse monoclonal anti-N-cadherin (1:500 BioLegend), and then developed following the conventional technique (Soler et al. 1997). The images were obtained in a Leica TCS SP8 inverted confocal laser-scanning microscope.

3.9 Blood components analysis

As one of the markers of systemic inflammation, the quantification of the cellular blood components was carried out. 500 µL of blood samples from each group were collected from jugular vein, and stored in BD Microtainer® tubes with ethylenediamine tetra-acetic acid (K_2EDTA) as anticoagulant. The following blood components were analyzed: white blood cells (WBC), monocytes (MID), granulocytes (GRA), lymphocytes (LY), red blood cells (RBC), and platelet (PLT), using a hematology auto analyzer (Abott Diagnostics Cell-Dyn 1700).

3.10 Statistical analysis

Data were collected from triplicates of eight independent experiments. A normal distribution by Kolmogorov-Smirnov's test was applied. One-way analysis of variance (ANOVA) followed by a Tukey's test were used to detect differences among treatments. The Kruskal-Walli's nonparametric test followed by *post hoc* Bonferroni's test, with Mann-Whitney's U correction test, were all used for comparison between two or more groups of non-normal

data, using the GraphPad 5 software. Values were considered of statistical significance at $p<0.05$.

4. Results

4.1 AgNPs characterization

TEM and DLS analysis revealed that AgNPs have spherical and pseudospherical shapes (Figure 1A), displaying a slight narrow size distribution with a mean particle size of 9.0 ± 2.0 nm for the hydrodynamic diameter (Figure 1B). The diameter obtained by TEM was 3.0 ± 1.5 nm. The particles zeta potential was -30.0 ± 10 mV, confirming its stability, since particles with positive zeta potential values above +30 mV or negative values below -30 mV are considered stable (Meléndrez et al. 2010). The values of this characterization are shown in Figure 1C.

4.2 AgNPs treatment increased BBB permeability, and was partially reversed by a pre-administration of Zn

We found that the experimental group treated with AgNPs during 24 h increased the content of EB in the brain tissue (>2.0 µg/g of brain tissue), in comparison to the control (<0.5 µg/g of brain tissue), as a consequence of the increased BBB permeability. In contrast, the group treated with Zn alone did not show differences compared to the control, whereas a pre-administration of Zn partially blocked (1.7 µg/g of brain tissue) the effects induced by AgNPs on the BBB permeability (Figure 2).

4.3 AgNPs treatment decreased the claudin-5 expression

Since an increase in BBB permeability has been related with a decrease in TJs proteins (Rosas-Hernandez et al. 2013, 2015), we analyzed the expression of claudin-5 as a classic marker for BBB permeability (Tsukita and Furuse 1999). We found that AgNPs increased

the BBB permeability through a modified expression of claudin-5 compared to the control. Moreover, the pretreatment with Zn and further administration of AgNPs was not different to the AgNPs treatment (Figure 3).

4.4 AgNPs treatment increased MTs levels in brain tissue, and a pre-administration of Zn restored these levels

To assess the role of MTs in the BBB affected by AgNPs, their protein expression was measured in the brains of rats exposed to these treatments. We observed that the group of rats exposed to Zn alone showed an increase of MTs in comparison to the control ($p<0.05$), and the group of rats exposed to AgNPs also increased the MTs expression ($p<0.01$), whereas the pre-treatment with Zn plus the administration of AgNPs restored the expression levels of MTs to those observed with the group of Zn treatment (not different to the control values; Figure 4).

4.5 AgNPs increased the number of granulocytes in blood tissue, while the pre-administration of Zn prevented this effect

In order to evaluate the systemic damage induced by AgNPs and its association with the damage to the BBB permeability, we determined, through the blood analyses, the count of the following cellular elements: WBC, MID, GRA, LY, RBC and PLT. The AgNPs treatment induced a significant increase in the GRA values (3.0 k/µL) in comparison to the control (< 1.00 k/µL) (Figure 5C), whereas no changes were observed in the rest of leukocytes (Figure 5); neither RBC, nor PLT were modified in the presence of this treatment (Figure 6), a result that agree with previous reports (Laloy et al. 2014). Similarly, those cell lines were not affected by Zn or Zn+AgNPs treatments (Figures 5 and 6).

4.6 The AgNPs treatment induced degeneration of the nervous tissue, and this effect was partially prevented by a pre-administration of Zn

We found, through the hematoxylin-eosin (H&E) and Nomarski techniques, that the experimental group treated with AgNPs exhibited considerable damage at the level of the cortex tissue, causing vasogenic edema on the blood vessels of the cerebral cortex compared with the control and Zn treatments (H&E staining and differential interference contrast microscopy) (Figures 7A and B). The Cajal staining showed tissue destruction in cortex (Figure 8), and a lymphocytic infiltrate is inferred. Comparatively, the Zn pretreatment group showed a reduction of tissue damage than that observed with the single administration of AgNPs (Figures 7 and 8).

4.7 The Zn pre-administration increased the N-cadherin levels in brain cortex

Due to the preventive effects induced by the pre-treatment with Zn on the BBB permeability, we decided to evaluate the degree of expression of N-cadherin, observing that the expression of this protein was increased in the brain cortex in rats exposed to AgNPs after Zn exposure, compared with the control and the Zn and AgNPs treatments (Figure 9).

Discussion

In the present work, we investigated whether a pre-treatment with Zn could prevent the brain damage induced by an IP administration of AgNPs, firstly upon the BBB permeability, and the possible mechanisms involved. The size of AgNPs employed was below 10 nm, this information is relevant because it is known that smaller NPs exert higher cytotoxic effects (Kim et al. 2012; Eckhardt et al. 2013).

Herein we found that an IP administration of <10 nm AgNPs (15 mg/Kg) induced an increase of the BBB permeability, decreased the protein expression of claudin-5, increased MTs

expression and promoted nervous tissue degeneration after 24 hours of exposure. In addition, at the systemic level, we observed that AgNPs increased the granulocytes levels, but no other blood components compared to the control. This inflammatory effect could, in turn, influence the CNS physiology, including the BBB integrity (Hawkins 2005).

In this sense, *in vivo* studies revealed the toxic effect of AgNPs upon the BBB. Sharma et al. (2009) administered 60 nm AgNPs by different exposure routes to mice and rats by IP (50 mg/kg), intravenous (IV) (30 mg/kg), intracarotid (IC) (2.5 mg/kg), and intracerebroventricular (ICV) (20 µg/10µl), showing that after 4 h of exposure, AgNPs promoted a discrete increase in BBB permeability when the route of exposure was IP; however, when the administration was IV, IC and ICV, the AgNPs induced an important BBB permeability increase from 4 h to 24 h. Xu et al. (2015) examined the effect of AgNPs in rats after an intragastric administration during a two-week exposure scheme; rats were treated with AgNPs at low and high doses (1 and 10 mg/kg, body weight, respectively). Both dosages triggered neuron shrinkage, extra-vascular lymphocytes and a significant increase of IL-4. These authors suggested that AgNPs promoted neuronal effects associated with an inflammatory process. In this context, our data are in agreement with some of these studies (Sharma et al. 2009b, a; Xu et al. 2015), showing that AgNPs are capable to induce damage at the BBB level, according to the size, dose and route of administration. In the present work, we used a smaller size (< 10 nm) via IP route, based on the reports by Sharma et al., who mentioned that this route produced less damage in comparison to others (Sharma et al. 2009a, b). In addition, with recent data obtained by our research group, we have found that these AgNPs, at the dose and route used in this study, are capable of being stored in brain tissue (data in process). Taking into account this evidence, we developed a model of altered BBB by AgNPs (15 mg/kg), but using a dose at which the neuronal and systemic effects could be

reverted in a total or partial manner with Zn, as it has been described for this metal (Kim et al. 2015).

Previously, we reported that 7.8 nm AgNPs exert differential effects in function of different brain cell types. The exposure of AgNPs at different concentrations on astrocyte primary cultures and C6 glioma cell line showed that these NPs were more toxic to the C6 line (the malignant astrocytes) than astrocytes (Salazar-García et al. 2015), suggesting the presence of cell-specific mechanisms of action regulating the effects and interactions activated by AgNPs. Among the possible mechanisms involved, Luther et al. (2011) observed that primary cultured astrocytes survived after an exposure of 55 nm AgNPs, and this effect comprised an overexpression of MTs as a potential mechanism for cell survival. Based on this evidence, we decided to evaluate the role of MTs induced by Zn upon the BBB permeability damage induced by AgNPs.

In order to evaluate the protective role of Zn, 24 hours before the administration of AgNPs, the group 4 received IP dose of $ZnCl_2$ as (27 mg/kg). In parallel, the group 2 (Zn control) received only the IP dose of $ZnCl_2$ (27 mg/kg). We observed that Zn did not modify the BBB permeability, neither the expression of the claudin-5 protein. However, the pre-treatment with Zn and the subsequent administration of AgNPs showed a partial prevention upon the increase of the BBB permeability in comparison to the control as well as upon the tissue damage. In addition, this treatment did not restore the claudin-5 expression. However, when we evaluated the expression of N-cadherin in the brain tissue, we observed an increase in the expression of this protein in the group exposed to AgNPs with previous exposure to Zn. The function of the N-cadherin is not yet very clear in the BBB; however, it has been reported that it participates in early stages of the formation of this barrier (Gerhardt 1999). In addition, several studies suggest that N-cadherin plays indispensable role in the cellular responses to

brain injury through the induction of reactive astrogliosis and the consequent neuroprotection dependent on calcium signaling (pemaru et al. 2013), Therefore, our results suggest that the increase of N-cadherin might be due to a first step of re-establishment of the BBB function, while TJ are restored. This would explain why the Zn pretreatment apparently produced an increased damage at the BBB level with a higher expression of N-cadherin, but with the levels of claudin-5 still diminished.

Conversely, when we evaluated, at the systemic level the cellular elements of the blood in the presence or absence of AgNPs and/or Zn, we found that the experimental group 3 (AgNPs) increased around 3-fold the granulocyte levels in comparison to the control. The granulocyte alterations have been previously reported, specifically in human neutrophils exposed to AgNPs, suggesting that these NPs are associated to a granulocyte-mediated inflammatory process (Liz et al. 2015; Poirier et al. 2016).

Moreover, we observed that the groups of rats exposed to AgNPs with the Zn pre-administration, the GRA levels were not increased with respect to the control, suggesting that at the systemic level, Zn exerts a protective role as an anti-inflammatory agent. This finding agrees with the reported by Franciscato et al. (2011), who evaluated *in vivo* the toxic effects of mercury and the effectiveness of Zn in the prevention of biochemical changes induced by the first. This protective effect was achieved at the same dose of Zn (27 mg/kg) that we used in the present work. The ability of Zn to reduce inflammation has been reported by Kim et al. (2012), showing that this element can act as an intracellular reactive oxygen species (ROS) scavenger through the modulation of the cyclooxygenase-2 (COX-2) expression, reducing the generation of the pro-inflammatory prostaglandin.

In our study we observed that the Zn pre-administration partially prevented the damage induced by the AgNPs on BBB permeability, as well as on the brain cortex tissue, and was

capable also to attenuate the MTs overexpression enhanced by AgNPs, suggesting that AgNPs induced MTs as an adaptive mechanism to the injury in progress as result from the accumulation of various harmful effects such as oxidative stress and inflammation activated by AgNPs (Alessandrini et al. 2017). These effects suggest that the protective effect induced by Zn could be related in part to its anti-inflammatory properties (Kim et al. 2012; Garla et al. 2017), that was evidenced and associated with the decrease in the granulocyte levels.

The anti-inflammatory properties of Zn have been the most evidenced as the most relevant protective mechanism, Mbiydzenyuy et al. (2018) showed that the pre-treatment of Zn intravenously administered (30 mg/kg) attenuated the brain damage in an experimental model of Parkinsonism by preventing lipid peroxidation and preserving the levels of reduced glutathione and the antioxidant enzymes in the midbrain. In this line, 0.02% Zn in the drinking water prevented behavioral and cholinergic perturbations induced by arsenic exposure (Kumar and Reddy 2018). Oral administration of 15 ppm of Zn was also able to ameliorate alterations in neurogenic markers (nestin, Ki67, doublecortin (DCX), and 5-bromo-2'-deoxyuridine) which decreased in obese mice (Nam et al. 2017). Based on the above information, we suggest that Zn could directly protect not only against BBB disrupted permeability induced by AgNPs administration, but also through the amelioration of oxidative stress measured as the reduced-to-oxidized glutathione ratio, which has been well-demonstrated after AgNPs exposure in the brain (Skalska et al. 2016).

In summary, we provide evidence in the brain about the role of Zn on the protective actions against the deleterious effects of AgNPs when administered via IP. Further studies are needed to determine the precise mechanisms of action of Zn in the preventive events against the brain damage induced by AgNPs.

Acknowledgments

The authors thank to Francisco Javier Torres de la Rosa, José Fernando García de la Cruz and Edgar Rangel Lopez for their technical assistance. This work was supported by the grant C16-PIFI-09-08.08 and the National Council of Science and Technology Project 268769. Samuel Salazar was recipient of a scholarship from CONACyT (342918).

Figure legends

Figure 1. AgNPs exhibited spherical and pseudospherical shapes, and are poly-disperse. TEM micrographs showing the polygonal shape of the AgNPs dispersed in water (A), and the corresponding size distribution obtained by DLS (B) are shown. The data obtained by the characterization are shown in the table (C).

Figure 2. AgNPs treatment increased BBB permeability, and was partially reversed by a pre-administration of Zn. Male Wistar rats were exposed to different treatments; EB dye extravasation was taken as an index of BBB permeability. The results are expressed as mean ± SEM (n=8 animals per group). *p<0.05, **p<0.01 vs control.

Figure 3. AgNPs treatment decreased the expression of claudin-5. Male Wistar rats were exposed to different treatments. The expression of claudin-5 was detected at 23 kDa (A). Densitometric analysis of the western blots was performed using ImageJ software (B). The results are expressed as mean ± SEM (n=8 animals per group). *p<0.05 vs control.

Figure 4. AgNPs treatment increased MT levels in brain tissue, while a pre-administration of Zn re-established these levels. Male Wistar rats were exposed to different treatments. The expression of MTs polymerized (FL-61 sc 11377) was detected at 17 kDa (A). Densitometric analysis of the western blots was performed using ImageJ software (B). The results are expressed as mean ± SEM (n=8 animals per group). *p<0.05 vs control.

Figure 5. AgNPs treatment increased granulocyte levels blood, while a pre-administration of Zn re-established these levels. Male Wistar rats were exposed to different treatments. Leukocytes (A), lymphocytes (B), granulocytes (C) and MID (D) were counted in peripherally blood. The results are expressed as mean ± SEM (n=8 animals per group). *p<0.05 vs control.

Figure 6. AgNPs treatment did not modify erythrocyte or platelet levels. Male Wistar rats were exposed to different treatments. Erytrocyte (A) and platelet levels (B) were counted in peripherally blood. The results are expressed as mean ± SEM (n=8 animals per group).

Figure 7. AgNPs treatment induced degeneration of the nervous tissue and was partially prevented by a pre-administration of Zn. Male Wistar rats were exposed to different treatments. Histological changes in the brain were observed using H & E staining (Panel A) and Differential interference contrast (Nomarski) (Panel B).

Figure 8. AgNPs treatment induced degeneration of the nervous cells and was partially prevented by a pre-administration of Zn. Male Wistar rats were exposed to different treatments. The morphology of nerve cells was observed using Cajal's staining.

Figure 9. The Zn pre-administration increases the levels of N-cadherin in brain cortex. Male Wistar rats were exposed to different treatments. The expression of N-cadherin was detected using mouse monoclonal anti N-cadherin antibody.

Figure 1

A)

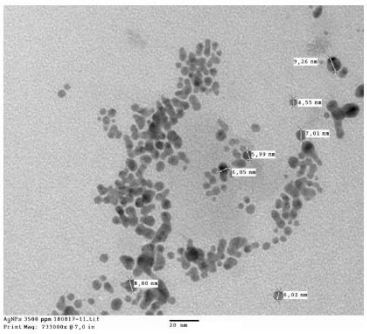

B)

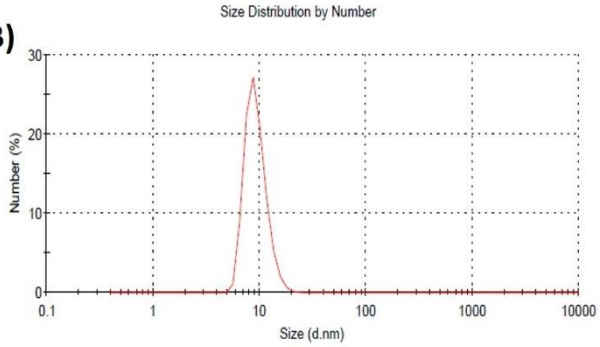

C)

Diameter DLS (nm)	Shape TEM	Diameter TEM (nm)	Zeta potential±ZD (mV)
9.0±2.0	Spherical and pseudospherical	3.0±1.5	-30±10

Figure 2

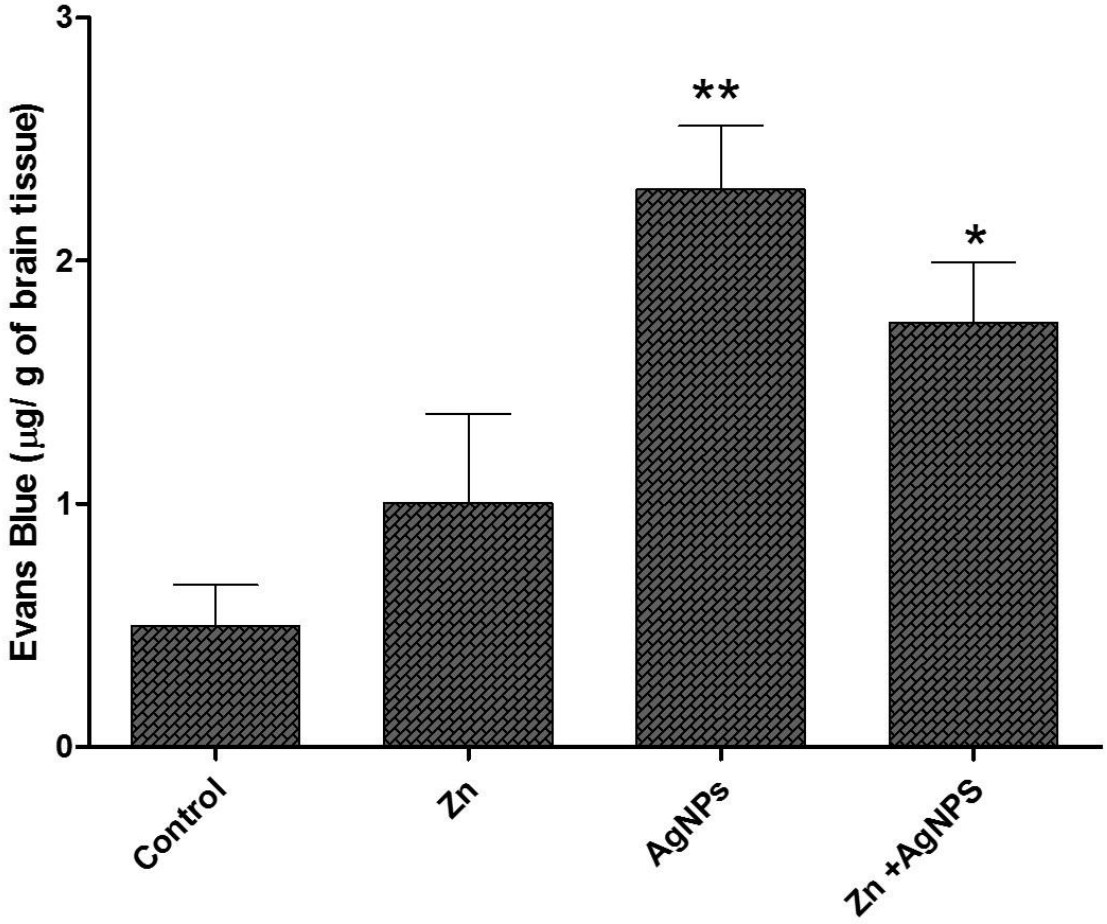
Evans Blue (μg/ g of brain tissue)
3
2
1
0
**
*
Control
Zn
AgNPs
Zn +AgNPS

Figure 3

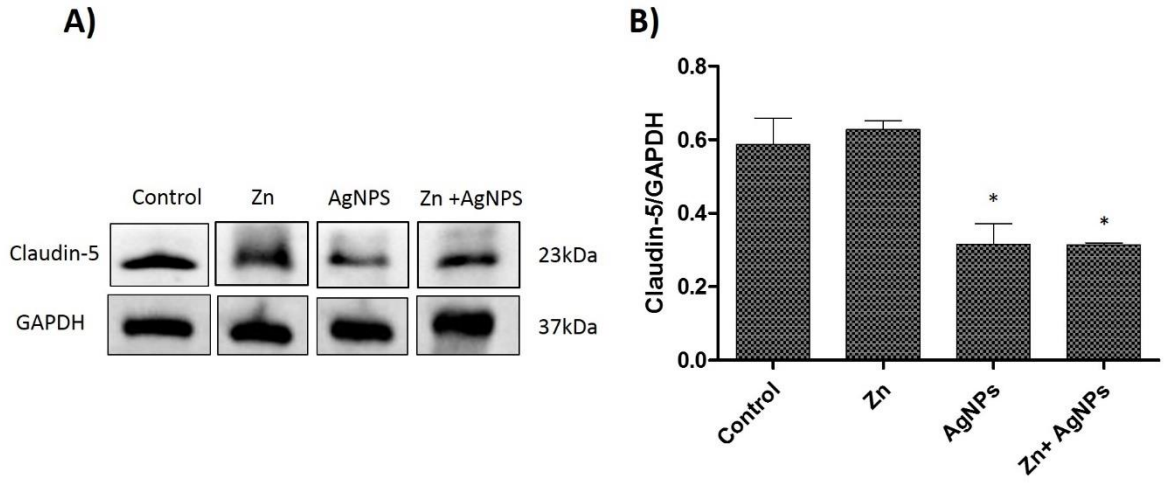
A)
Control
Zn
AgNPS
Zn +AgNPS
Claudin-5
GAPDH
23kDa
37kDa
B)
Claudin-5/GAPDH
0.8
0.6
0.4
0.2
0.0
*
*
Control
Zn
AgNPs
Zn+ AgNPs

Figure 4

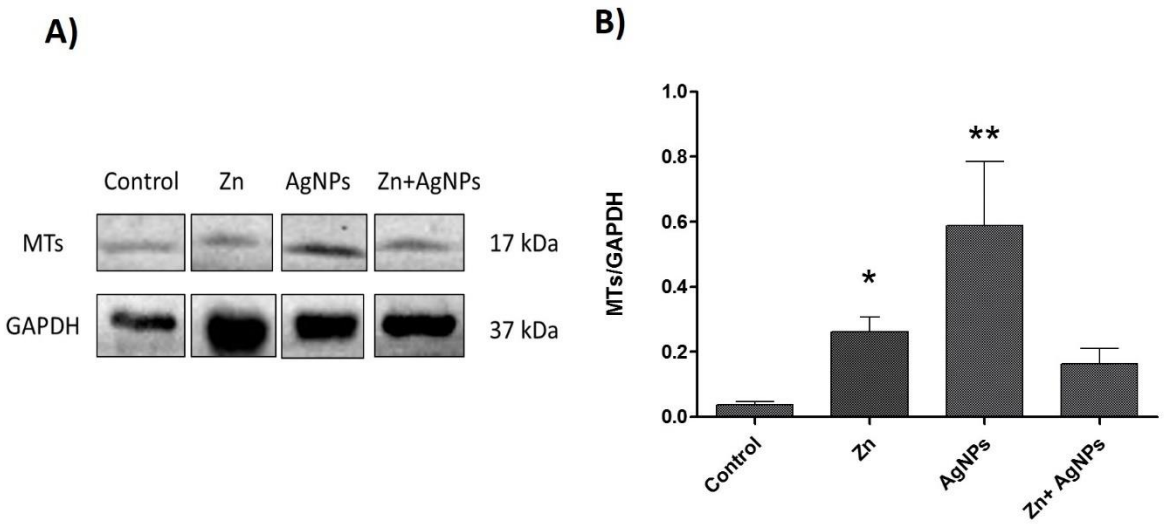
A)
Control
Zn
AgNPs
Zn+AgNPs
MTs
17 kDa
GAPDH
37 kDa
B)
MTs/GAPDH
1.0
0.8
0.6
0.4
0.2
0.0
*
**
Control
Zn
AgNPs
Zn+ AgNPs

Figure 5

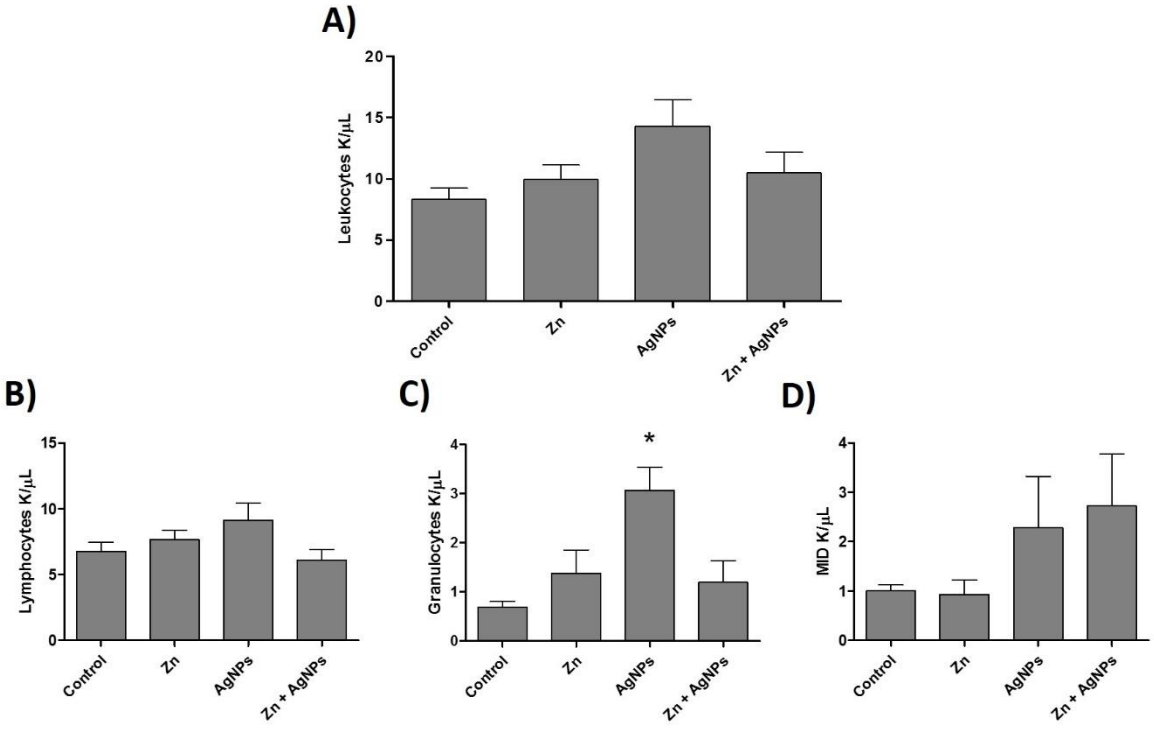
A)
Leukocytes K/µL
20
15
10
5
0
Control
Zn
AgNPs
Zn + AgNPs
B)
Lymphocytes K/µL
15
10
5
0
Control
Zn
AgNPs
Zn + AgNPs
C)
Granulocytes K/µL
*
4
3
2
1
0
Control
Zn
AgNPs
Zn + AgNPs
D)
MID K/µL
4
3
2
1
0
Control
Zn
AgNPs
Zn + AgNPs

Figure 6

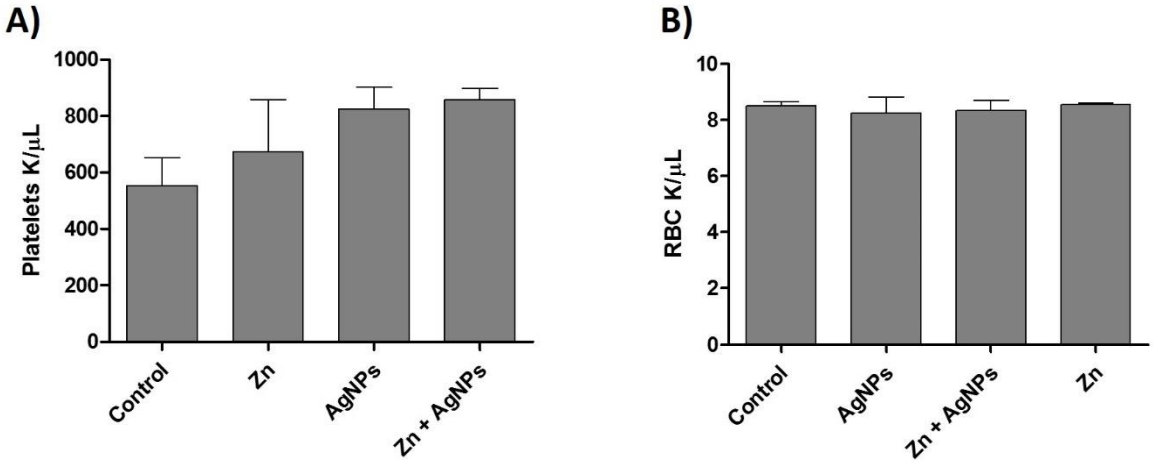
A)
Platelets K/µL
1000
800
600
400
200
0
Control
Zn
AgNPs
Zn + AgNPs
B)
RBC K/µL
10
8
6
4
2
0
Control
AgNPs
Zn + AgNPs
Zn

Figure 7

PANEL A

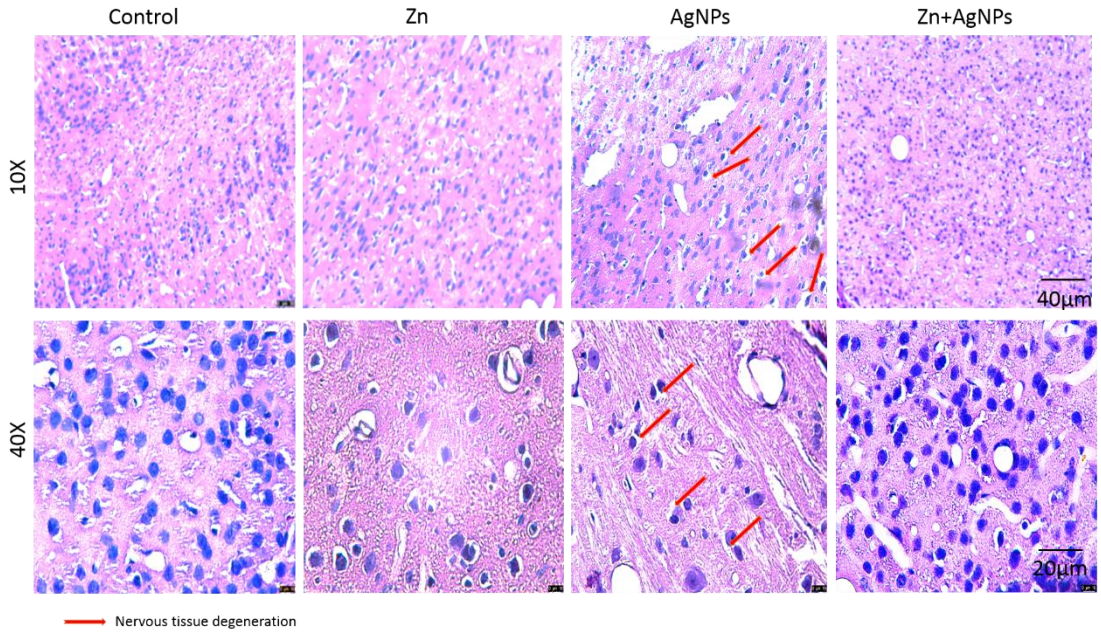

Figure 7

PANEL B

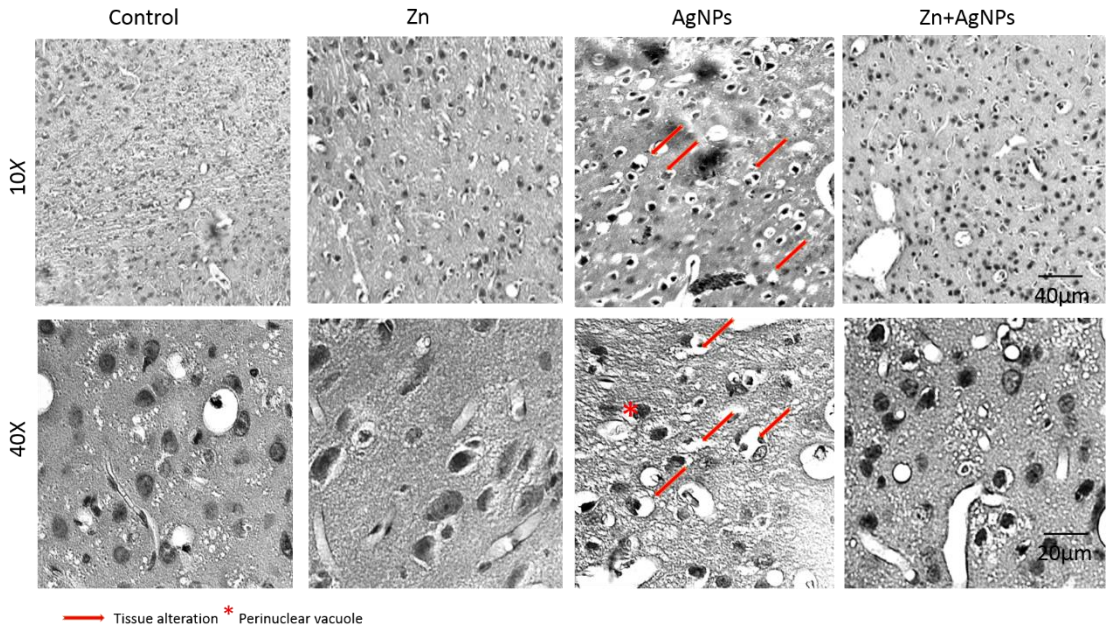

Figure 8

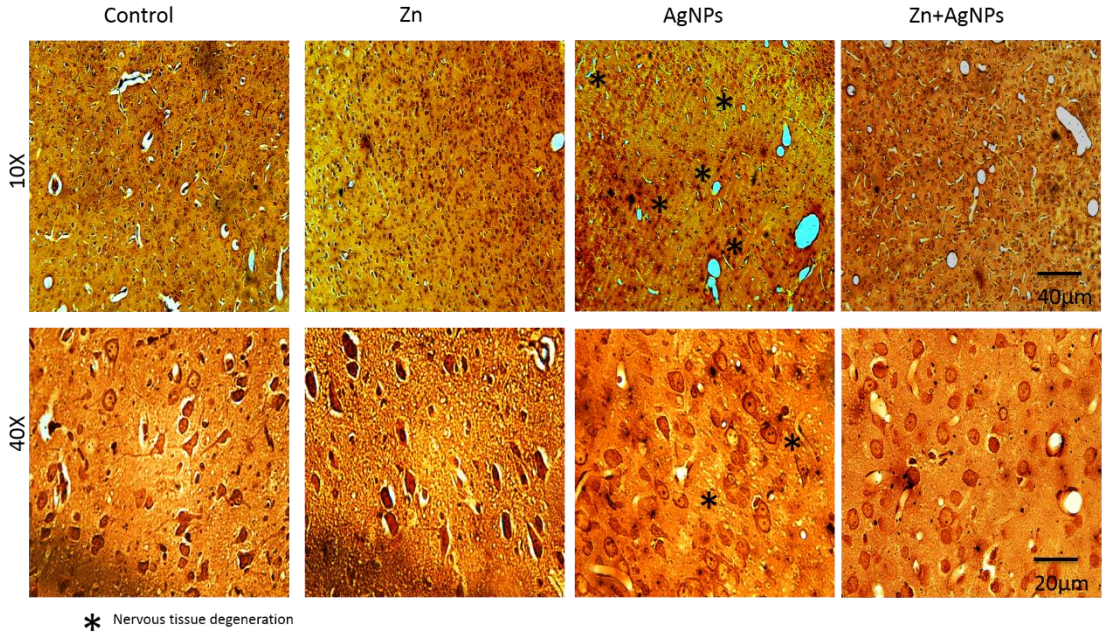
Control
Zn
AgNPs
Zn+AgNPs
10X
40X
40µm
20µm
Nervous tissue degeneration

Figure 9

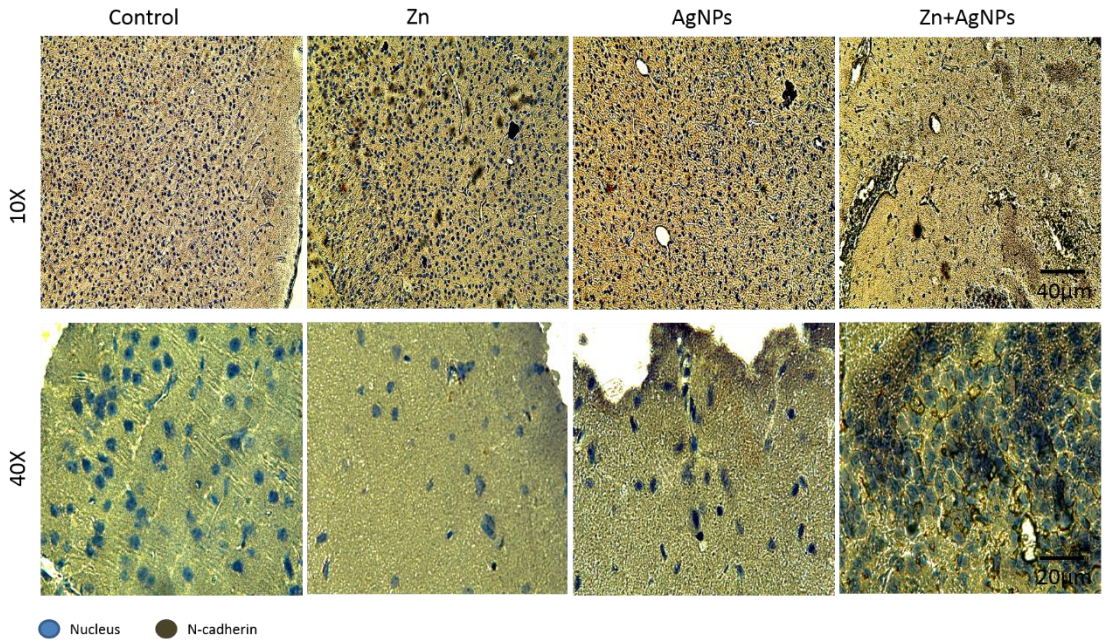
Control
Zn
AgNPs
Zn+AgNPs
10X
40X
40µm
20µm
Nucleus
N-cadherin

Conflict of interest

The authors declare that they have no conflict of interest.

References

Alessandrini F, Vennemann A, Gschwendtner S, et al (2017) Pro-Inflammatory versus Immunomodulatory Effects of Silver Nanoparticles in the Lung: The Critical Role of Dose, Size and Surface Modification. Nanomaterials. doi: 10.3390/nano7100300

AshaRani P, Hande MP, Valiyaveettil S (2009) Anti-proliferative activity of silver nanoparticles. BMC Cell Biol 10:65. doi: 10.1186/1471-2121-10-65

Baiomy AA, Attia HF, Soliman MM, Makrum O (2015) Protective effect of ginger and zinc chloride mixture on the liver and kidney alterations induced by malathion toxicity. Int J Immunopathol Pharmacol. doi: 10.1177/0394632015572083

British Standards Institution (2007) Terminology for nanomaterials. Publicly Available Specif 16. doi: 9780580613210

Chen X, Schluesener HJ (2008) Nanosilver: A nanoproduct in medical application. Toxicol Lett 176:1–12. doi: 10.1016/j.toxlet.2007.10.004

Coyle P, Philcox JC, Carey LC, Rofe AM (2002) Metallothionein: The multipurpose protein. Cell Mol Life Sci 59:627–647. doi: 10.1007/s00018-002-8454-2

Eckhardt S, Brunetto PS, Gagnon J, et al (2013) Nanobio silver: Its interactions with peptides and bacteria, and its uses in medicine. Chem. Rev.

Espinosa-Cristobal LF, Martinez-Castañon GA, Loyola-Rodriguez JP, et al (2013) Toxicity, distribution, and accumulation of silver nanoparticles in Wistar rats. J Nanoparticle Res 15:. doi: 10.1007/s11051-013-1702-6

Franciscato C, Moraes-Silva L, Duarte FA, et al (2011) Delayed biochemical changes

induced by mercury intoxication are prevented by zinc pre-exposure. Ecotoxicol Environ Saf 74:480–486. doi: 10.1016/j.ecoenv.2010.11.011

Garla R, Kango P, Gill NK, Garg ML (2017) Induction of Metallothionein in Rat Liver by Zinc Exposure: A Dose and Time Dependent Study. Protein J 36:433–442. doi: 10.1007/s10930-017-9737-7

Gerhardt H (1999) N-cadherin expression in endothelial cells during early angiogenesis in the eye and brain of the chicken: Relation to blood-retina and blood-brain barrier development. Eur J Neurosci. doi: 10.1046/j.1460-9568.1999.00526.x

Gliga a R, Skoglund S, Wallinder IO, et al (2014) Size-dependent cytotoxicity of silver nanoparticles in human lung cells: the role of cellular uptake, agglomeration and Ag release. Part Fibre Toxicol 11:11. doi: 10.1186/1743-8977-11-11

Gonzalez C, Rosas-Hernandez H, Ramirez-Lee MA, et al (2016) Role of silver nanoparticles (AgNPs) on the cardiovascular system. Arch Toxicol 90:493–511. doi: 10.1007/s00204-014-1447-8

Hawkins BT (2005) The Blood-Brain Barrier/Neurovascular Unit in Health and Disease. Pharmacol Rev 57:173–185. doi: 10.1124/pr.57.2.4

Huber JD, Witt KA, Hom S, et al (2001) Inflammatory pain alters blood-brain barrier permeability and tight junctional protein expression. Am J Physiol Circ Physiol. doi: 10.1152/ajpheart.2001.280.3.H1241

Ioachim EE, Kitsiou E, Carassavoglou C, et al (2000) Immunohistochemical localization of metallothionein in endometrial lesions. J Pathol. doi: 10.1002/1096-9896(2000)9999:9999<::AID-PATH616>3.0.CO;2-Q

Kanemaru K, Kubota J, Sekiya H, et al (2013) Calcium-dependent N-cadherin up-regulation mediates reactive astrogliosis and neuroprotection after brain injury. Proc Natl Acad

Sci. doi: 10.1073/pnas.1300378110

Kim J, Kim S, Jeon S, et al (2015) Anti-inflammatory effects of zinc in PMA-treated human gingival fibroblast cells. Med Oral Patol Oral Cir Bucal. doi: 10.4317/medoral.19896

Kim TH, Kim M, Park HS, et al (2012) Size-dependent cellular toxicity of silver nanoparticles. J Biomed Mater Res - Part A 100 A:1033–1043. doi: 10.1002/jbm.a.34053

Kumar MR, Reddy GR (2018) Influence of age on arsenic-induced behavioral and cholinergic perturbations: Amelioration with zinc and α-tocopherol. Hum Exp Toxicol. doi: 10.1177/0960327117698540

Laloy J, Minet V, Alpan L, et al (2014) Impact of Silver Nanoparticles on Haemolysis, Platelet Function and Coagulation. Nanobiomedicine. doi: 10.5772/59346

Liu P, Huang Z, Chen Z, et al (2013) Silver nanoparticles: A novel radiation sensitizer for glioma? Nanoscale 5:11829–11836. doi: 10.1039/c3nr01351k

Liu W, Worms IAM, Herlin-Boime N, et al (2017) Interaction of silver nanoparticles with metallothionein and ceruloplasmin: Impact on metal substitution by Ag(i), corona formation and enzymatic activity. Nanoscale 9:6581–6594. doi: 10.1039/c7nr01075c

Liz R, Simard JC, Leonardi LBA, Girard D (2015) Silver nanoparticles rapidly induce atypical human neutrophil cell death by a process involving inflammatory caspases and reactive oxygen species and induce neutrophil extracellular traps release upon cell adhesion. Int Immunopharmacol 28:616–625. doi: 10.1016/j.intimp.2015.06.030

Luther EM, Koehler Y, Diendorf J, et al (2011) Accumulation of silver nanoparticles by cultured primary brain astrocytes. Nanotechnology 22:. doi: 10.1088/0957-4484/22/37/375101

Luther EM, Schmidt MM, Diendorf J, et al (2012) Upregulation of metallothioneins after

exposure of cultured primary astrocytes to silver nanoparticles. Neurochem Res 37:1639–1648. doi: 10.1007/s11064-012-0767-4

Meléndrez MF, Cárdenas G, Arbiol J (2010) Synthesis and characterization of gallium colloidal nanoparticles. J Colloid Interface Sci. doi: 10.1016/j.jcis.2009.11.069

Nam SM, Kim JW, Kwon HJ, et al (2017) Differential Effects of Low- and High-dose Zinc Supplementation on Synaptic Plasticity and Neurogenesis in the Hippocampus of Control and High-fat Diet-fed Mice. Neurochem Res. doi: 10.1007/s11064-017-2353-2

Oberdörster G, Oberdörster E, Oberdörster J (2005) Nanotoxicology: An emerging discipline evolving from studies of ultrafine particles. Environ Health Perspect 113:823–839. doi: 10.1289/ehp.7339

Poirier M, Simard JC, Girard D (2016) Silver nanoparticles of 70 nm and 20 nm affect differently the biology of human neutrophils. J Immunotoxicol 13:375–385. doi: 10.3109/1547691X.2015.1106622

Rosas-Hernandez H, Cuevas E, Lantz S, et al (2013) Prolactin and Blood-Brain Barrier Permeability. Curr Neurovasc Res 10:278–286. doi: 10.2174/15672026113109990025

Rosas-Hernandez H, Ramirez M, Ramirez-Lee MA, et al (2015) Inhibition of prolactin with bromocriptine for 28days increases blood-brain barrier permeability in the rat. Neuroscience 301:61–70. doi: 10.1016/j.neuroscience.2015.05.066

Ruttkay-Nedecky B, Nejdl L, Gumulec J, et al (2013) The role of metallothionein in oxidative stress. Int J Mol Sci 14:6044–6066. doi: 10.3390/ijms14036044

Salazar-García S, Silva-Ramírez AS, Ramirez-Lee MA, et al (2015) Comparative effects on rat primary astrocytes and C6 rat glioma cells cultures after 24-h exposure to silver nanoparticles (AgNPs). J Nanoparticle Res 17:1–13. doi: 10.1007/s11051-015-3257-1

Sharma HS, Ali SF (2006) Alterations in blood-brain barrier function by morphine and

methamphetamine. Ann N Y Acad Sci 1074:198–224. doi: 10.1196/annals.1369.020

Sharma HS, Ali SF, Hussain SM, et al (2009a) Influence of Engineered Nanoparticles from Metals on the Blood-Brain Barrier Permeability, Cerebral Blood Flow, Brain Edema and Neurotoxicity. An Experimental Study in the Rat and Mice Using Biochemical and Morphological Approaches. J Nanosci Nanotechnol 9:5055–5072. doi: 10.1166/jnn.2009.GR09

Sharma HS, Ali SF, Tian ZR, et al (2009b) Chronic treatment with nanoparticles exacerbate hyperthermia induced blood-brain barrier breakdown, cognitive dysfunction and brain pathology in the rat. Neuroprotective effects of nanowired-antioxidant compound H-290/51. J Nanosci Nanotechnol 9:5073–5090. doi: 10.1166/jnn.2009.GR10

Skalska J, Dąbrowska-Bouta B, Strużyńska L (2016) Oxidative stress in rat brain but not in liver following oral administration of a low dose of nanoparticulate silver. Food Chem Toxicol. doi: 10.1016/j.fct.2016.09.026

Soler a P, Harner GD, Knudsen K a, et al (1997) Expression of P-cadherin identifies prostate-specific-antigen-negative cells in epithelial tissues of male sexual accessory organs and in prostatic carcinomas. Implications for prostate cancer biology. Am J Pathol. doi: 10.1002/adma.201300292

Trickler WJ, Lantz SM, Murdock RC, et al (2010) Silver nanoparticle induced blood-brain barrier inflammation and increased permeability in primary rat brain microvessel endothelial cells. Toxicol Sci 118:160–170. doi: 10.1093/toxsci/kfq244

Tsukita S, Furuse M (1999) Occludin and claudins in tight-junction strands: Leading or supporting players? Trends Cell Biol 9:268–273. doi: 10.1016/S0962-8924(99)01578-0

Wen J, Qian S, Yang Q, et al (2014) Overexpression of netrin-1 increases the expression of

tight junction-associated proteins, claudin-5, occludin, and ZO-1, following traumatic brain injury in rats. Exp Ther Med. doi: 10.3892/etm.2014.1818

Xu L, Shao A, Zhao Y, et al (2015) Neurotoxicity of Silver Nanoparticles in Rat Brain After Intragastric Exposure. J Nanosci Nanotechnol 15:4215–4223. doi: 10.1166/jnn.2015.9612

Zlokovic B V. (2008) The Blood-Brain Barrier in Health and Chronic Neurodegenerative Disorders. Neuron 57:178–201. doi: 10.1016/j.neuron.2008.01.003

Capítulo 2

Silver nanoparticles (AgNPs) and zinc chloride ($ZnCl_2$) exposure order determines the toxicity in C6 rat glioma cells

Resumen en inglés

Silver nanoparticles (AgNPs) induced specific cell toxicity, and they are used as a tool for the study of several pathologies such as cancer. This work aimed to elucidate the toxic effect of < 10-nm silver nanoparticles (AgNPs) and zinc chloride ($ZnCl_2$) in different administration orders on C6 rat glioma cells, as a biological model of study. C6 rat glioma cells were exposed to increasing concentrations of AgNPs (10–100 μg/mL) in the presence or absence of ZnCl2 (10–50 μg/mL) for 24 h. AgNPs or $ZnCl_2$ as separate treatments decreased C6 rat glioma cell viability by 21% and 13%, respectively, versus the control, using the MTT assay. The administration of AgNPs (50 μg/mL) in the presence of $ZnCl_2$ (10–50 μg/mL) was performed under two conditions: as pretreatment and as concomitant administration; both of them showed a significant decrease in the cell viability, around 30% and 90%, respectively. It was the concomitant treatment, which exerted the most significant effect on the viability decrease. We also observed that 24-h exposure to AgNPs increased cell populations (40%) in stages G0/G1 of the cell cycle, and decreased the number of cells (60%) in stages G2/M. However, in the concomitant treatment, as well as during induced cell death, the $ZnCl_2$ pretreatment and concomitant treatment modified the cycle, increasing the S phase by 10%, suggesting that zinc (Zn) could be an essential regulator of the C6 rat glioma cell damage induced by AgNPs. This study will allow us to understand the mechanisms of cellular response to AgNPs, for the eventual study of these particles as a potential agent against cancer, such as glioblastoma multiforme.

Resumen en español

Las nanopartículas de plata (AgNPs) inducen toxicidad celular específica y se utilizan como herramienta para el estudio de diversas patologías como el cáncer. Este trabajo tuvo como objetivo dilucidar el efecto tóxico de nanopartículas de plata (AgNPs) de <10 nm y cloruro de zinc ($ZnCl_2$) en diferentes órdenes de administración en células de glioma de rata C6, como modelo biológico de estudio. Se expusieron células de glioma de rata C6 a concentraciones crecientes de AgNPs (10 a 100 μg/mL) en presencia o ausencia de $ZnCl_2$ (10 a 50 μg/mL) durante 24 h. Las AgNPs o el $ZnCl_2$ como tratamientos separados disminuyeron la viabilidad de las células de glioma de rata C6 en un 21% y un 13%, respectivamente, en comparación con el control, utilizando el ensayo MTT. La administración de AgNP (50 μg/mL) en presencia de $ZnCl_2$ (10-50 μg/mL) se realizó bajo dos condiciones: como pretratamiento y como administración concomitante; ambos mostraron una disminución significativa en la viabilidad celular, alrededor del 30% y 90%, respectivamente. Fue el tratamiento concomitante el que ejerció el efecto más significativo sobre la disminución de la viabilidad. También observamos que la exposición de 24 h a AgNP aumentó las poblaciones de células (40%) en las etapas G0/G1 del ciclo celular, y disminuyó el número de células (60%) en las etapas G2/M. El pretratamiento con $ZnCl_2$ y el tratamiento concomitante modificaron el ciclo celular, aumentando la fase S en un 10%, lo que sugiere que el zinc (Zn) podría ser un regulador esencial en el daño inducido por las AgNPs en células de glioma de rata C6. Este estudio permitirá comprender los mecanismos de respuesta celular a las AgNPs, para un eventual estudio de estas partículas como potencial agente contra el cáncer, como el glioblastoma multiforme.

Silver nanoparticles (AgNPs) and zinc chloride ($ZnCl_2$) exposure order determines the toxicity in C6 rat glioma cells

Samuel Salazar-Garcia[a,b], José Fernando Garcia-Rodrigo[a,b], Gabriel A. Martínez-Castañon[c], Victor Manuel Ruiz-Rodríguez[b], Diana Patricia Portales-Perez[a,b], Carmen Gonzalez[a,b].

[a]Universidad Autonoma de San Luis Potosí, Facultad de Ciencias Quimicas, San Luis Potosi, Mexico.

[b]Universidad Autonoma de San Luis Potosi, Centro de Investigacion en Ciencias de la Salud y Biomedicina. San Luis Potosi, Mexico.

[c]Universidad Autonoma de San Luis Potosi, Facultad de Estomatologia, San Luis Potosi, Mexico

Corresponding author:

Carmen Gonzalez, Ph. D.

Universidad Autonoma de San Luis Potosi

Facultad de Ciencias Quimicas

Av. Dr. Manuel Nava Núm. 6.

Zona Universitaria. Zip Code 78210

San Luis Potosí, México.

Phone: 011-52-444-8262440 Ext. 6459

Email: gonzalez.castillocarmen@uaslp.mx

cgonzalez.uaslp@gmail.com

1. Abstract

This work aimed to elucidate the toxic effect of <10 nm silver nanoparticles (AgNPs) and zinc chloride ($ZnCl_2$) in different administration orders on C6 rat glioma cells, employed as a biological model to study and elucidate the potential toxicity mechanisms of action of nanomaterials (NMs). C6 rat glioma cells were exposed to increasing concentrations of AgNPs (10-100 μg/mL) in the presence or absence of $ZnCl_2$ (10-50 μg/mL) for 24 h. AgNPs or $ZnCl_2$ as separate treatments decreased C6 rat glioma cell viability by 21% and 13%, respectively, versus the control, using the MTT assay. The administration of AgNPs (50 μg/ml) in the presence of $ZnCl_2$ (10-50 μg/ml) was performed under two conditions; as pretreatment and as concomitant administration, both of them showed a significant decrease in the cell viability, around 30% and 90%, respectively. They were the concomitant treatment, which exerted the most significant effect on the viability decrease. We also observed that 24 h exposure to AgNPs increased cell populations (40 %) in stages G0/G1 of the cell cycle, and decreased the number of cells (60 %) in stages G2/M. However, in the concomitant treatment, as well as during induced cell death, the $ZnCl_2$ pretreatment and concomitant treatment modified the cycle, increasing the S phase by 10%, suggesting that zinc (Zn) could be an essential regulator of the C6 rat glioma cells damage induced by AgNPs.

Keywords: Silver nanoparticles, Zinc Chloride, Glioblastoma multiforme.

2. Introduction

Nanotechnology is defined as the use and application of nanomaterials (NMs), which in turn are defined as materials having one or more external dimensions with at least one dimension in the range of 1 to 100 nanometers (British Standards Institution 2007). Silver nanoparticles (AgNPs) have widely used in biological and industrial applications. It has been reported that AgNPs exert a variety and controversial biological effects, depending on their size, concentration, shape, biological target, and route of exposure (Liu et al. 2017). The AgNPs display multiple effects linked to genotoxicity, such as alterations in the cell cycle, through events that lead the cell to its division, duplication, necrosis and/or apoptosis, are actively reported in several *in vitro* and *in vivo models* during the years (Salazar-García et al. 2015; Fouad and Hafez 2018). Therefore, AgNPs are potential candidates to study multiple pharmacological approaches. For example, as an anticancer agent, however, it is necessary to explore in-depth the range of physiological effects and/or protective mechanisms that some cells could confer and trigger when NMs agents like AgNPs are exposed to them. Studies, in this sense, remain elusive.

The cells can respond to different metal detoxifying mechanisms due to the metallic nature of AgNPs. The Zn is an essential metallic agent which acts as a cofactor regulating physiological effects (Maret 2013), that activates metal detoxifying mechanisms, some of them, mediated by protein complex such as metallothioneins (Ruttkay-Nedecky et al. 2013). Besides, Zn acts as an anti-inflammatory agent, through stabilizing the actin filaments of neurons (Perrin et al. 2017), promoting a protective role to the cell in the presence of metallic nature toxic substances, such as AgNPs (Chen et al. 2006; Luther et al. 2012). At the same time, Zn has been shown to decrease cancer progression likely by reducing angiogenesis and induction of inflammatory cytokines while increasing apoptosis in cancer cells (Prasad et al.

2009). This work aimed to evaluate *in vitro,* the toxicity and cell cycle progression of AgNPs on C6 glioma cells and to determine whether this toxicity was modified by pretreatment or simultaneous exposure to $ZnCl_2$.

3. Materials and methods

3.1 Chemical

AgNPs were synthesized by Gabriel Martinez-Castañon, Ph.D. from Universidad Autonoma de San Luis Potosi. Other compounds, such as bovine serum albumin (BSA), penicillin/streptomycin, Hoechst, $ZnCl_2$, H_2O_2, and 3-(4, 5-dimethylthiazol- 2-yl)-2,5-diphenyltetrazolium bromide (MTT), and propidium iodide acquired from Sigma-Aldrich Company (St. Louis, MO, USA). Dulbecco's Modified Eagle's Medium (DMEM) and Alexa Fluor 488 anti-rabbit secondary antibody acquired from Invitrogen (Carlsbad, CA, USA). Cisplatin purchased from Laboratorios PISA (Mexico City).

3.2 Synthesis of AgNPs

AgNPs were synthesized as previously described (Espinosa-Cristobal et al., 2013). AgNPs with spherical shape were synthesized from a 0.35 M $AgNO_3$ solution placed in a 250 mL reaction vessel. Under magnetic stirring, 10 mL of deionized water containing gallic acid (0.1 g) was added to 100 mL of the Ag+ solution. After the addition of gallic acid, the pH of the solution was adjusted to 11 with 1.0 M NaOH. Afterward, the solution was heated for 30 min at 80 °C, and the final concentration of AgNPs used for *in vitro* treatments was 3,500 μg/mL (Ruttkay-Nedecky et al. 2013).

3.3 AgNPs characterization

AgNPs were characterized using dynamic light scattering (DLS) assay to determine particle size. Size assay was performed using a DLS Malvern Zetasizer Nano ZS (Instruments Worcestershire, United Kingdom) operated with a He–Ne laser at a wavelength of 633 nm

and a detection angle of 90°; all samples were analyzed during 60 s at 25 °C. The zeta potential was measured in Dulbecco's Modified Eagle Medium (DMEM) and in deionized water (DW) at 37 °C for 24 h to verify the stability of the particles in the solution in where the AgNPs treatment conditions were done. By confirming the shape, each sample was diluted in DMEM and DW. Then 50 µL of each suspension was placed on a copper grid for transmission electron microscopy (TEM) using a JEOL JEM-1230 microscope at an accelerating voltage of 100 kV. VIS–NIR spectroscopy (CHEMUSB4-VIS–NIR Ocean optics) was performed to determine the position of the surface plasmon resonance.

3.4 C6 rat glioma cell line

Glioblastoma cells were cultured and expanded in Petri dishes in the presence of DMEM supplemented with 10% FBS, penicillin (100 units / mL) and streptomycin (0.1 mg / mL) at 37 ° C and 5% CO_2 until confluence (Doblas et al. 2010; Silva-Ramirez et al. 2018). Cells were reseeded in 6 and 96-well plates (10 000 cells per well) and incubated in supplemented DMEM at 37 ° C and 5% CO_2 until reaching a confluence of 90% before applying the treatments. C6 rat glioma cell line was obtained from the American Type Culture Collection (ATCC-CCL- 107^{TM}, Manassas, VA).

3.5 Cell viability assays

Cell viability was colorimetrically determined using 3 (4, 5-dimethylthiazol-2-yl) -2, 5-diphenyltetrazol bromide or MTT, based on the metabolic reduction of this dye through the mitochondrial succinate-dehydrogenase to a colored compound (formazan) detected at an optical density of 590 nm. The number of viable cells was proportional to the amount of formazan produced (Denizot and Lang 1986). Cells were exposed to increasing concentrations of $ZnCl_2$ (10, 25 or 50 µg / mL) for 24 h, AgNPs (10, 25, 50 or 100 µg / mL) for 24 h and; AgNPs (50 µg/mL) for 24h with $ZnCl_2$ (10 to 50 µg/mL) pretreatment or

concomitant exposure. Hydrogen peroxide 2% (H_2O_2) was used as a positive control of dead, and cisplatin (75 µg/mL) was used as an antineoplastic control. The treated cell cultures were incubated with 10% MTT for four h at 37 ° C, followed by the addition of 100 µL of dimethyl sulfoxide (DMSO) and incubation for 10 min at room temperature. The optical density was determined at 590 nm in a bio rad iMark ® plate reader.

3.6 Flow cytometry

The stages of the cell cycle were determined according to the nuclear DNA content by flow cytometry. The C6 rat glioma cells in a number of $2.5x10^5$ cells were seeded and incubated in 24-well plates and then incubated in the presence of the different AgNPs treatments for 24 h. Subsequently, the medium was removed, and cells were resuspended in 0.5 mL of Propidium iodide (IP) buffer (1mg / ml sodium citrate, 50 µg / ml propidium iodide (Sigma-Aldrich), 0.3% Triton X-100 and 40 µg / ml RNAse), and incubated for 30 min in the dark. After, the cells were gently resuspended mechanically (pipetting) and placed in a Falcon® 5 ml round-bottom polystyrene tube covered with light, and immediately analyzed in the FACSCantoII flow cytometer (BD Bioscience, San Diego, CA). The data were analyzed using the FACS Diva software. The results were expressed as the percentage of cells in G0/G1 (normal diploid DNA phase), S (DNA synthesis phase), and G2/M (mitosis phase), as previously reported (Moreno-Vilet et al. 2014), and the FACS Diva software was used to analyze the data.

3.7 Lactate dehydrogenase assay

The evaluation of cell death index by necrosis was performed using a colorimetric assay based on the measurement of lactate dehydrogenase (LDH) activity released from the cytosol of damaged cells into the supernatant (Bopp and Lettieri 2008). According to the manufacturer instructions and after the respective treatments, 100 µL of the supernatants

were collected, and the reactive mixture was added and incubated for 30 min at room temperature in the dark. The LDH activity was quantified colorimetrically through the measurement of absorbance at 490 nm. The Bio-Rad microplate spectrophotometer (Hercules, CA, USA) was used. Values were represented as percent of control.

3.8 Cell morphology

After the exposure to the treatments described above, the cells were captured and observed in the bright field using a Motic inverted microscope equipped with a Moticam Pro 205A camera at 20X.

3.9 Statistical analysis

Data were collected from triplicates of three independent experiments. After confirmation of normal distribution by the Kolmogorov–Smirnov's test, a one-way analysis of variance (ANOVA) followed by a Tukey post hoc test was used to detect differences among treatments. Statistical analysis was performed using the Statistica 7.0 software package (StatSoft, Tulsa, OK, USA), whereas Graph Pad Prism V 7.3 (Graph- Pad Software Inc.) was used for data plotting.

4. Results

4.1 AgNPs characterization

The TEM and DLS analysis revealed that AgNPs in DW and DMEM acquired spherical and pseudospherical shapes (Figure 1A, 1C), and exhibited a slight narrow size distribution with a mean particle size of 9.34±2.25 nm and 8.34±1.50 nm for the hydrodynamic diameter (Figure 1B, 1D) respectively. TEM diameter and zeta potential values were 4.83±2.99 nm/-30.6±16.3 mV in DW and 4.88±2.22 nm/-12.2±12.8 mV in DMEM. The plasmon resonance value was 415 nm for both media. The extended values of this characterization shown in Table 1.

4.2 $ZnCl_2$ reduces the cell viability on C6 rat glioma cells.

To evaluate the effect of $ZnCl_2$ on the viability of C6 rat glioma cells, increasing concentrations of $ZnCl_2$ (10, 25, and 50 μg/mL) during 24 h were prepared and tested. Figure 2A shows that $ZnCl_2$ significantly decreased the cell viability only at a concentration of 50 μg/mL in comparison to the control. This effect at this concentration was similar to that induced by cisplatin, an antineoplastic control, and less potent than the hydrogen peroxide. Figures 2B and 2C show a bright-field micrograph of the morphology of C6 rat glioma cells. The untreated cells displayed the classic morphology of these immortalized cells with long, branched protrusions (Figure 2B). Morphology of the cells treated in the presence of $ZnCl_2$ at 25μg/mL was damaged (Figure 2C), and their disposition and organization were altered, suggesting that $ZnCl_2$ promoted this disruption.

4.3 AgNPs reduce cell viability on C6 rat glioma cells

It has been reported that the *in vitro* exposure of C6 rat glioma cells to AgNPs with a diameter of <10 nm decreased their viability (Salazar et al. 2015). We confirmed and reproduced this finding previously reported via the MTT assay. C6 rat glioma cells were treated in the presence of increasing concentrations of AgNPs < 10 nm (10, 25, 50, and 100 μg/mL) for 24 h. Figure 3A shows that only the concentrations of 50 and 100 μg/mL of AgNPs significantly decreased the mitochondrial activity of C6 rat glioma cells in comparison to the control. The effect of 100 μg/ml AgNPs was comparable to that induced by cisplatin and, both concentrations of AgNPs (50 and 100 μg/mL) were less potent in comparison to hydrogen peroxide. Figure 3B and 3C show in bright-field micrograph the morphology of C6 rat glioma cells. The untreated cells display the classic morphology of these immortalized cells with long, branched protrusions (Figure 3B). However, cells treated in the presence of 50 μg/mL

AgNPs (Figure 3C), exerted a similar morphology to that observed in the presence of $ZnCl_2$ (Figure 2C), finding an alteration in their organization and disposition again.

4.4 AgNPs in the presence of $ZnCl_2$ (24 h pretreatment) reduces the cell viability of C6 rat glioma cells drastically compared to individual treatments

Due to our previous work reported on the protective role of Zn against metallic agents such as silver (Franciscato et al. 2011). Increasing concentrations of $ZnCl_2$ (0- 50 μg/mL) and a unique concentration of 50 μg/mL AgNPs. Figure 4A shows a significant cell viability reduction following combined treatments in comparison to the control. We observed that AgNPs in the presence of $ZnCl_2$ (24 h pretreatment) induced a significant reduction of mitochondrial activity of C6 rat glioma cells in comparison to the control. The most prominent effect was observed when a concentration of 50 μg/ml $ZnCl_2$ was used, as the decrease in mitochondrial activity reached almost 82% compared to the control. This effect was comparable to H_2O_2 exposure (Figure 4A). The bright-field micrograph of C6 rat glioma cells treated in the presence of $ZnCl_2$ 25 μg/mL and 50 μg/mL AgNPs showed total damage of C6 rat glioma cells; the cells lost their classical morphology. They showed cellular debris (Figure 4C) in comparison to the control (Figure 4B).

4.5 *AgNPs in the presence of $ZnCl_2$ in a concomitant treatment reduced the cell viability of C6 rat glioma cells more than AgNPs with 24h $ZnCl_2$ pretreatment.*

When the viability of cells exposed to the concomitant treatment of $ZnCl_2$ and AgNPs was evaluated, we observed a significant reduction in cell viability (90%), compared to that observed with single administrations. This decrease in viability was around 15% and 25% (Figure 5A), more than that observed with only Zn pretreatment at the same concentrations (Figure 4A). The Bright-field micrograph of C6 rat glioma cells treated in the presence of 25 μg/mL $ZnCl_2$ and 50 μg/mL AgNPs concomitant, showed total damage of C6 rat glioma

cells. The cells lost their typical morphology and showed cellular debris (Figure 5C) in comparison to the control (Figure 5B). A comparison between pretreatment and concomitant treatment shown in Figure 6.

4.6 AgNPs in the presence and absence of $ZnCl_2$ modify the cell cycle of C6 rat glioma cells

Due to the concomitant treatment of AgNPs and Zn reduced the viability, the pretreatment with Zn and subsequent AgNPs exposure partially decreased the cell viability, we decided to evaluate if these treatments and the administration order could modify the cell cycle of C6 rat glioma cells. The population of cells at different stages of the cell cycle during 24 h was not altered by a single administration of zinc (25 μg/mL). In contrast, the population of cells exposed to a concentration of 50 μg/mL of AgNPs increased in the G0/G1 phase (Figure 7A), and decreased in the G2 phase (Figure 7C). In the case of cells exposed to both Zn and AgNPs under the preadministration and concomitant order, the cell populations increased in the G0/G1 phase (Figure 7A). They decreased again in the G2 phase (Figure 7C). This effect was similar to the culture condition in the presence of AgNPs only. However, a key difference was that in Zn treatments (preadministration and concomitant order), an increase of cell populations in phase S was identified (Figure 7B).

4.7 AgNPs in the presence of $ZnCl_2$ 24 h pretreatment and single administration induce cell death of C6 rat glioma cells

The measurement of the LDH activity as a marker of cell damage was done to investigate whether this one could be the responsible to the decrement on the C6 rat glioma cells viability or stirring in the cell cycle when the cells were treated with AgNPs and/or $ZnCl_2$. We found single administration of AgNPs, and the concomitant treatment of AgNPs and $ZnCl_2$ increased the levels of LDH in comparison to the control. In contrast, the sole administration of $ZnCl_2$ and the pretreatment of $ZnCl_2$ and AgNPs did not modify these levels (Figure 8).

5. Discussion

The purpose of this work was to investigate the effect of AgNPs < 10 nm and $ZnCl_2$ on C6 rat glioma upon the cell viability, progression of the cell cycle, and cell death. The size of AgNPs used was below 10 nm because it has been reported that NPs smaller than 10 nm exert higher cytotoxic effects (Kim et al. 2012).

We found that individual treatments with $ZnCl_2$ or AgNPs reduced the cell viability of the C6 rat glioma cells after 24 h. Additionally, concomitant treatment with $ZnCl_2$ and AgNPs significantly reduced the viability of the C6 rat glioma cells in comparison to the individual treatments. The administration of both agents Zn and AgNPs exerted a significant reduction in the cell viability when a concomitant administration was done in contrast to the condition in where Zn was administrated 24 hours before the AgNPs exposure. Besides, all the groups exposed to AgNPs showed an increase of cells in the stages G0/G1 and a decrease of cells in the G2/M; also, the cells that received both agents (AgNPs/$ZnCl_2$) showed an increase of cells in the S phase. And when the cell death was evaluated through the LDH assay, an increase in this effect was observed when the C6 rat glioma cells were exposed to a single administration of AgNPs and concomitant administration of Zn and AgNPs, however the preadministration of Zn and posterior exposure to AgNPs did not induce death.

To date, there are limited studies related to the mechanisms of cell damage induced by AgNPs and $ZnCl_2$. Here, we evaluated the effect of AgNPs with or without Zn, and the impact that this kind of treatment could confer on C6 glioma cells. In this sense, we have observed that AgNPs *per se* induced a toxic effect on glioma cells, while $ZnCl_2$ could play a pivotal role against the treatment with AgNPs depending on the order of exposure of both agents.

The data showed that the order of the treatments is essential in the viability and toxicity of C6 rat glioma cells; when a co-treatment with AgNPs and $ZnCl_2$ was done, we observed a

decrease in viability up to 95% that was greater than the preadministration of the subsequent exposure to AgNPs. It is essential to highlight that when $ZnCl_2$ was pre-administered 24 hours before the AgNPs, the harmful effect was significantly lower than that exerted when the co-treatment AgNPs-$ZnCl_2$ was done, suggesting that the order of the Zn administration influences and increases the toxicity of AgNPs upon the C6 glioma cells. Few studies have displayed the toxic effect and the protective role of Zn in different biological models. *In vivo* studies have shown that nanoparticles can generate several responses depending on their size, shape, concentration, cellular target, and the exposure route among cell lines. Previously, we reported that differential effects occurred between astrocytes and C6 rat glioma cells when they were exposed to AgNPs <10 nm. In astrocytes, the AgNPs induced a programmed cell death process, meanwhile in the altered form of astrocytes (C6 rat glioma cells) was promoted a nonspecific process through necrosis.

On the other hand, Urbaska et al., 2015 described that AgNPs 70 nm (40 μg/mL) promoted a higher antiproliferative activity than the antiapoptotic effect in a model of human GBM. Also, the AgNPs 6-20 nm decreased the ATP content, caused by mitochondrial damage, and increased the reactive oxygen species (ROS) due to the rupture of the respiratory chain, since the AgNPs have been located inside the organelles; the nucleus and the mitochondria, then their direct involvement in the mitochondrial impairment and DNA damage. These results are positively related to ours since, as mentioned above, a reduction in the mitochondrial activity of the C6 rat glioma cells was observed when they were exposed to AgNPs <10 nm (Figure 3).

An *in vitro* study carried out by Beljanski et al., 1994 showed the differential effects exerted by astrocytic cells and GBM when they were treated with metals such as Zn, demonstrating that at concentrations of 1 to 25 μg/mL of $ZnCl_2$ increased in 30% the number of astrocytic

cells to their control. In contrast, in our work, we found that the C6 rat glioma cells, which at concentrations ranging from 25 to 100 μg/mL of $ZnCl_2$, decreased the cell multiplication up to 75% versus the control (Beljanski and Crochet 1994). Many of the human cancers are associated with the absence of the expression of p53 or its mutant expression (mtp53). Puca et al., 2011 described how Zn could restore sensitivity to therapeutic drugs and inhibits tumor growth by reactivating the mutant p53.

Among the few reports published about Zn and AgNPs in diseases such as cancer, Priyadharshini et al., 2014 examined the anticancer activity of 65 nm AgNPs and 95 nm Zinc oxide nanoparticles (ZnONP) against human prostate cancer (PC3), concluding that ZnONPs exhibit higher anticarcinogenic activity against the PC3 cell line than AgNPs,

The cell cycle is a vital process defined as a series of events that lead the cell to its division and duplication. (Mahmoudi et al. 2011). Several studies have shown that AgNPs are capable of altering the progression of the cell cycle due to possible cytotoxicity mechanisms that compromise the progress of the cycle to the next stage. For instance in human lung fibroblast and human glioblastoma, the AgNPs induced an arrest of the cell population in phases G2/M after a 48-hour exposure, that in consequence promote in the cells mitochondrial disruption with the interruption of the ATP synthesis that could eventually damage the DNA (AshaRani et al. 2009). Similarly, in our work, we have observed a decrease in the cell population in the G2/M phase. An increase in the G1/G0 phase, detecting an increase of cells in the S phase when they are exposed to Zn, suggesting that Zn could activate the DNA synthesis process, which in turn counteracting the DNA damage caused by the AgNPs.

In summary, the present work shows that both $ZnCl_2$ and AgNPs as independent treatments decrease mitochondrial activity by 13% and 21%, respectively. Additionally, a common treatment with $ZnCl_2$ and AgNPs decreased the mitochondrial activity more significantly and

abruptly than the individual treatments. Furthermore, it was observed that under the procedures as mentioned above, a reduction in the number of C6 glioma cells was demonstrated. This work highlights the effect of AgNPs and $ZnCl_2$ exposure on the survival of C6 glioma cells as a study target to elucidate the potential toxicity mechanisms of action of nanomaterials.

The rational of this study was to try and put in context the toxic effect induced by AgNPs, and whether this toxic effect could be altered or protected by other metallic physiologic cofactors such as zinc. As well, is important to evaluate the fine mechanisms of action through the AgNPs induced toxicity in these kinds of cells. And moreover, to generate knowledge that impact at long time in the designs of bio tools or nano drugs directed in the combat to the brain cancer.

More studies are being carried out to determine new avenues for understanding the specific mechanisms of action that make the survival of C6 glioma cells vulnerable to exposure to AgNPs and Zn.

Acknowledgments

This work was supported by the grant C16-PIFI-09-08.08. Samuel Salazar was the recipient of scholarships from CONACyT (342918). And CONACYT- SINANOTOX PN-2017-01-4710, recipient: Carmen Gonzalez PhD.

6. Conflict of interest

None**.**

7. Figure legends

Figure 1. AgNPs have spherical and pseudospherical shapes and are poly-disperse.

TEM micrographs showing the spherical and pseudospherical shape of the AgNPs (A, C) and their correspondent size distribution obtained by DLS dispersed in DW (B) and DMEM (D). The data collected by the characterization are shown in table 1.

Figure 2. $ZnCl_2$ decreased cell viability in C6 rat glioma cells.

Cells were treated with increasing concentrations (10, 25, and 50 μg/mL) of $ZnCl_2$ for 24 h. The mitochondrial activity was assessed by MTT assay. One-way analysis of variance (ANOVA) followed by Tukey post hoc test ***$p<0.001$ was performed versus control of C6 rat glioma cells. Each value represents the mean ± SEM (A). Bright-field micrography characterization of C6 rat glioma cells under control (B) and (25 μg/mL) $ZnCl_2$ treatments (C).

Figure 3. AgNPs reduce cell viability on C6 rat glioma cells.

Cells were treated with increasing concentrations (10, 25, 50, and 100 μg/mL) of AgNPs for 24 h. The mitochondrial activity was assessed by MTT assay. One-way analysis of variance (ANOVA) followed by Tukey post hoc test ***$p<0.001$ was performed versus control of C6 rat glioma cells. Each value represents the mean ± SEM (A). Bright-field micrography characterization of C6 rat glioma cells under control (B) and (50 μg/mL) AgNPs treatments (C).

Figure 4. AgNPs in the presence of $ZnCl_2$ 24 h pretreatment reduces the cell viability of C6 rat glioma cells

Cells were treated with a unique concentration (50 μg/mL) of AgNPs for 24h with $ZnCl_2$ (0-50 μg/mL) 24 h pretreatment. Mitochondrial function was assessed by MTT assay. One-way analysis of variance (ANOVA) followed by Tukey post hoc test ***$p<0.001$ was performed versus control of C6 rat glioma cells. Each value represents the mean ± SEM (A). Bright-field micrography of C6 rat glioma cells under control treatment (B), and (50 μg/mL) AgNPs with (25 μg/mL) $ZnCl_2$ 24 h pretreatment (C).

Figure 5. Concomitant treatment of AgNPs + $ZnCl_2$ 24 h reduced the cell viability of C6 rat glioma cells

Cells were treated with a unique concentration (50 μg/mL) of AgNPs + (0-50 μg/mL) $ZnCl_2$ 24h treatment. Mitochondrial function was assessed by MTT assay. One-way analysis of variance (ANOVA) followed by Tukey post hoc test ***$p<0.001$ was performed versus control of C6 rat glioma cells. Each value represents the mean ± SEM (A). Bright-field micrography of C6 rat glioma cells under control treatment (B) and (50 μg/mL) AgNPs + (25 μg/mL) $ZnCl_2$ 24 h treatment (C).

Figure 6. Concomitant treatment reduces in a significant manner, the cell viability of C6 rat glioma cells versus pretreatment.

Mitochondrial function was assessed by MTT assay. One-way analysis of variance (ANOVA) followed by Tukey post hoc test ***$p<0.001$ was performed versus treatments. Each value represents the mean ± SEM.

Figure 7. The AgNPs in the presence and absence of $ZnCl_2$ modify the cell cycle of C6 rat glioma cells

The effect of AgNPs on the cell cycle of C6 rat glioma cells evaluated, as indicated in the material and methods section. The cells were treated for 24 h with (25 μg/mL) $ZnCl_2$, or (50 μg/mL) AgNPs, or (50 μg/mL) AgNPs with $ZnCl_2$ (25 μg/mL) 24 h pretreatment, as well as

the concomitant (25 μg/mL) $ZnCl_2$ + (50 μg/mL) AgNPs treatment. After the acquisition of the sample, it was analyzed the fluorescence intensity of PI. It was observed the subpopulations: G0/G1 cells, S cells, G2/M cells. Mean values of the percentage of IP from three independent experiments ± SEM are presented. Significant alterations are expressed relative to controls and marked with asterisks. Statistical significance was considered if * $p < 0.05$, ** $p < 0.01$ or *** $p < 0.001$.

Figure 8. AgNPs and concomitant treatment increased LDH leakage, and a $ZnCl_2$ pretreatment reduces this leakage in C6 rat glioma cells.

C6 cells rat glioma cells were treated with 25 μg/mL $ZnCl_2$, 50 μg/mL AgNPs or 50 μg/mL AgNPs with 25 μg/mL ZnCl (24 h pretreatment), as well as the concomitant 25 μg/mL $ZnCl_2$ 50 μg/mL AgNPs treatment. LDH leakage was estimated as an index of necrosis. A one-way ANOVA test with a post hoc Fisher's Least Significant Difference (LSD) test *$p<0.05$ or **$p<0.01$ were performed versus control of C6 rat glioma cells; $^{\&\&\&}p<0.001$ versus pretreatment. Each value represents the mean ± SEM.

Table 1. The Size, shape, zeta potential, and plasmon resonance of the two samples prepared with AgNPs.

8. Figures and Table

Table 1

Sample	Size TEM M ± SD (nm)	Shape TEM	Hydrodynamic diameter M ± SD (nm)	Zeta Potential (mV)	Plasmon
AgNPs *DW	4.83 ± 2.99	Spherical / Pseudospherical	9.34 ± 2.25	-30.6 ± 16.3	415 nm
AgNPs **DMEM	4.88 ± 2.22	Spherical / Pseudospherical	8.34 ± 1.50	-12.2 ± 12.8	415 nm

*Deionized Water, **Dulbecco's Modified Eagle Medium, M = Mean

Figure1

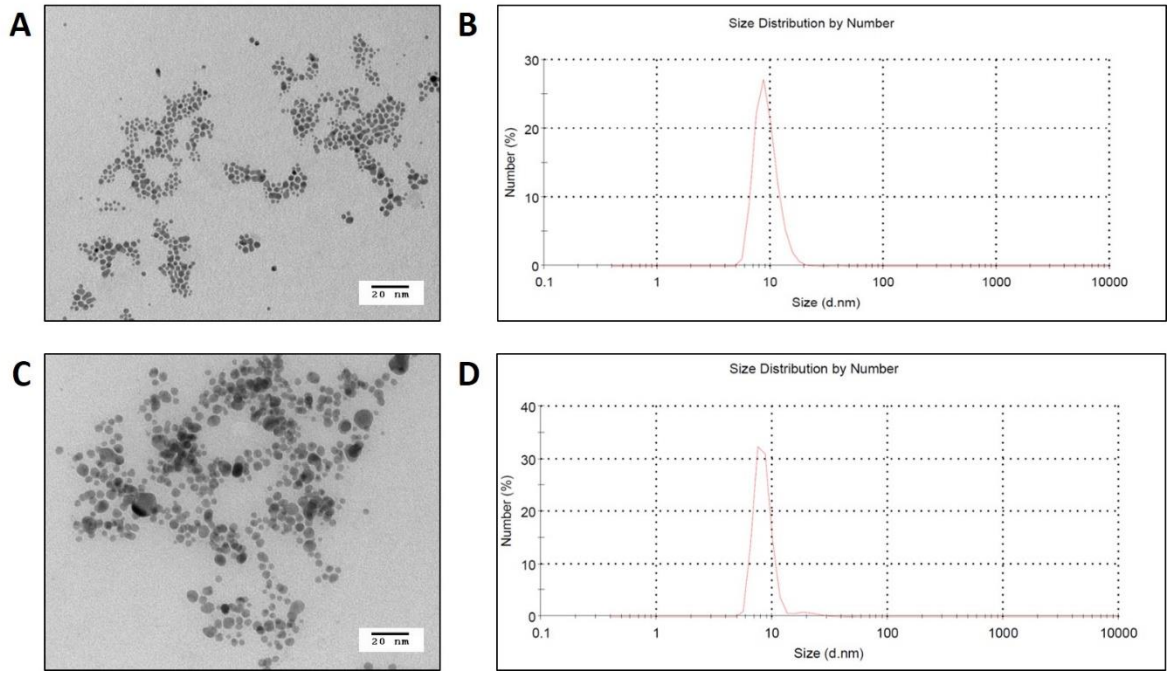
A
20 nm
B
Size Distribution by Number
Number (%)
Size (d.nm)
C
20 nm
D
Size Distribution by Number
Number (%)
Size (d.nm)

Figure2

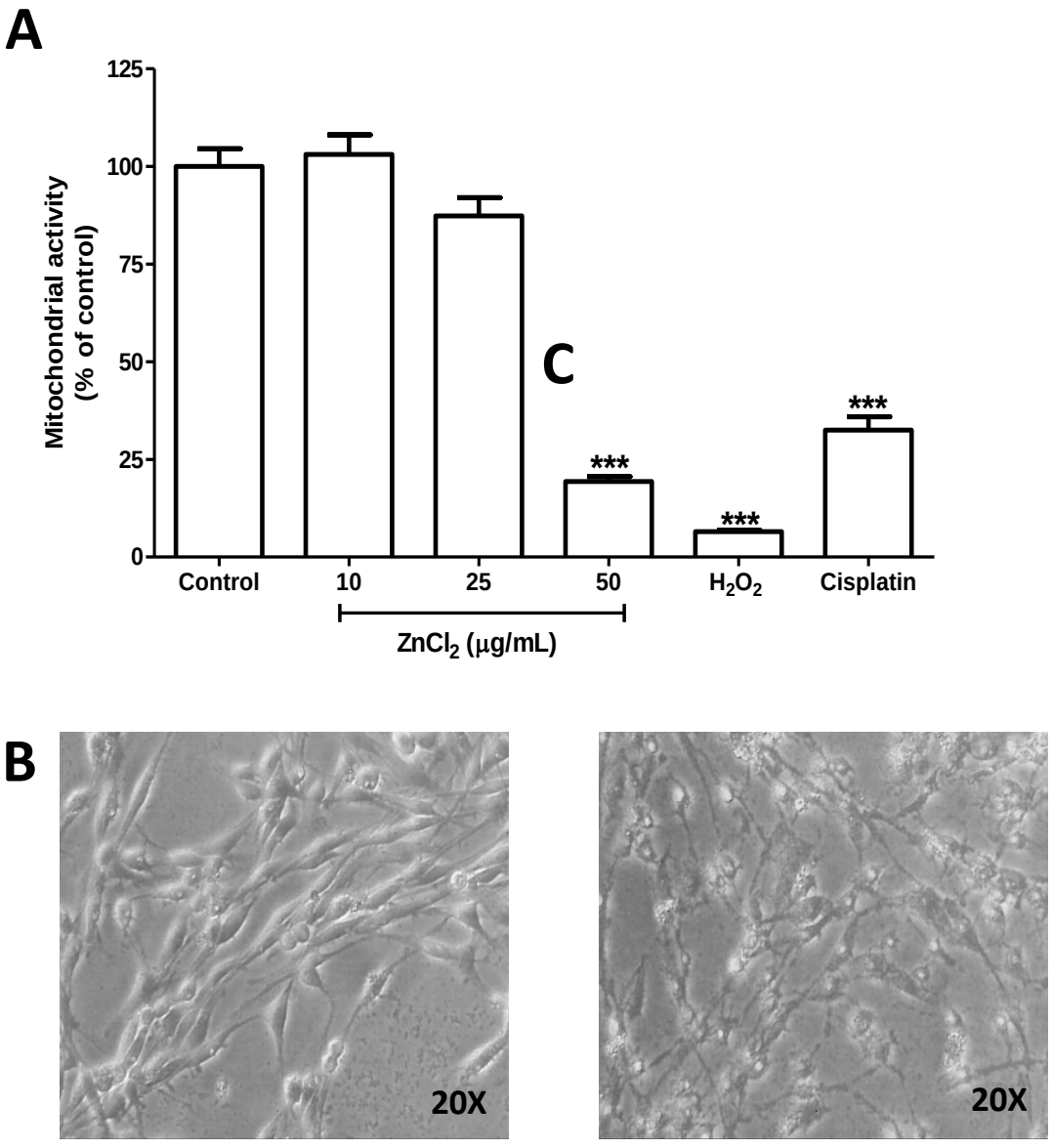
A
125
100
75
50
25
0
Mitochondrial activity
(% of control)
C
***
***
***
Control
10
25
50
H2O2
Cisplatin
ZnCl2 (μg/mL)
B
20X
20X

Figure 3

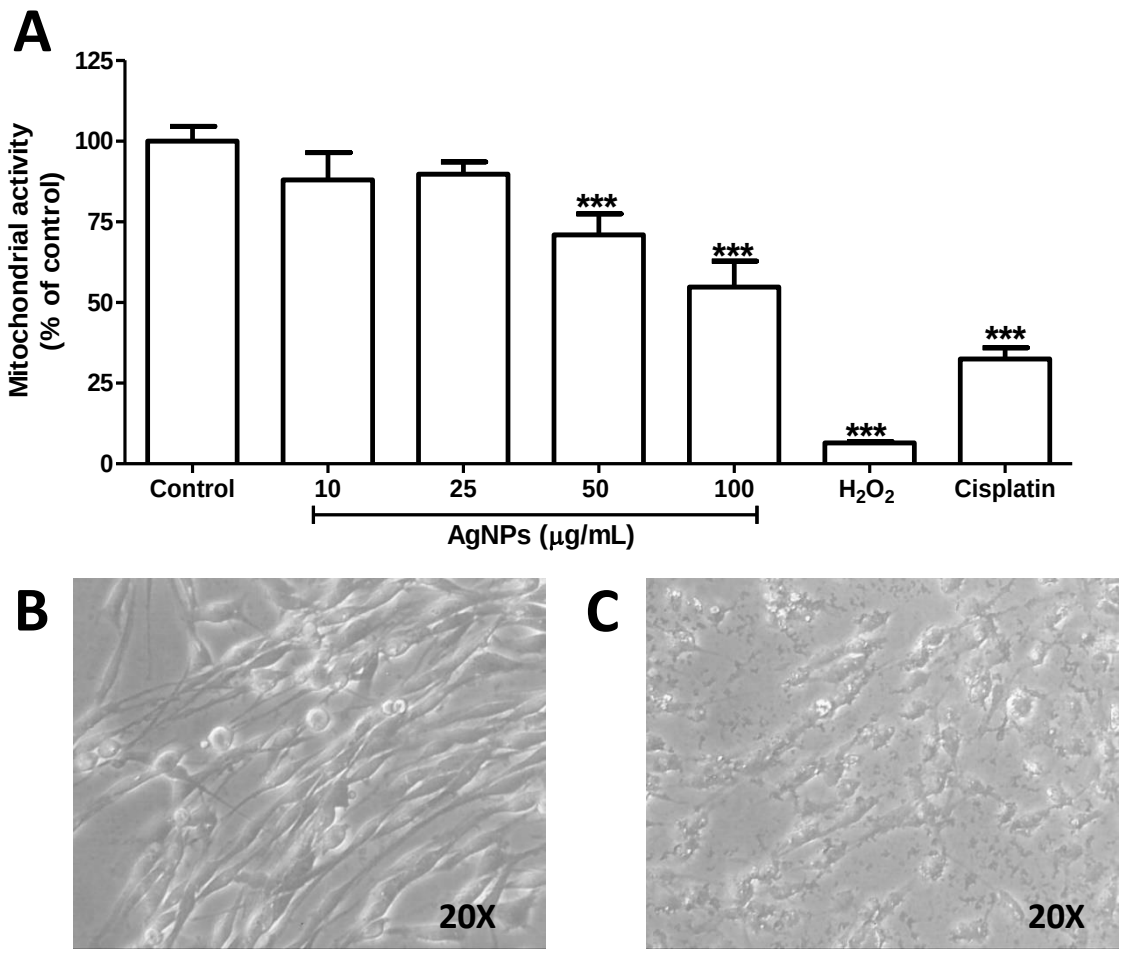
A
Mitochondrial activity (% of control)
125
100
75
50
25
0
***
***
***
***
Control
10
25
50
100
H2O2
Cisplatin
AgNPs (μg/mL)
B
20X
C
20X

Figure 4

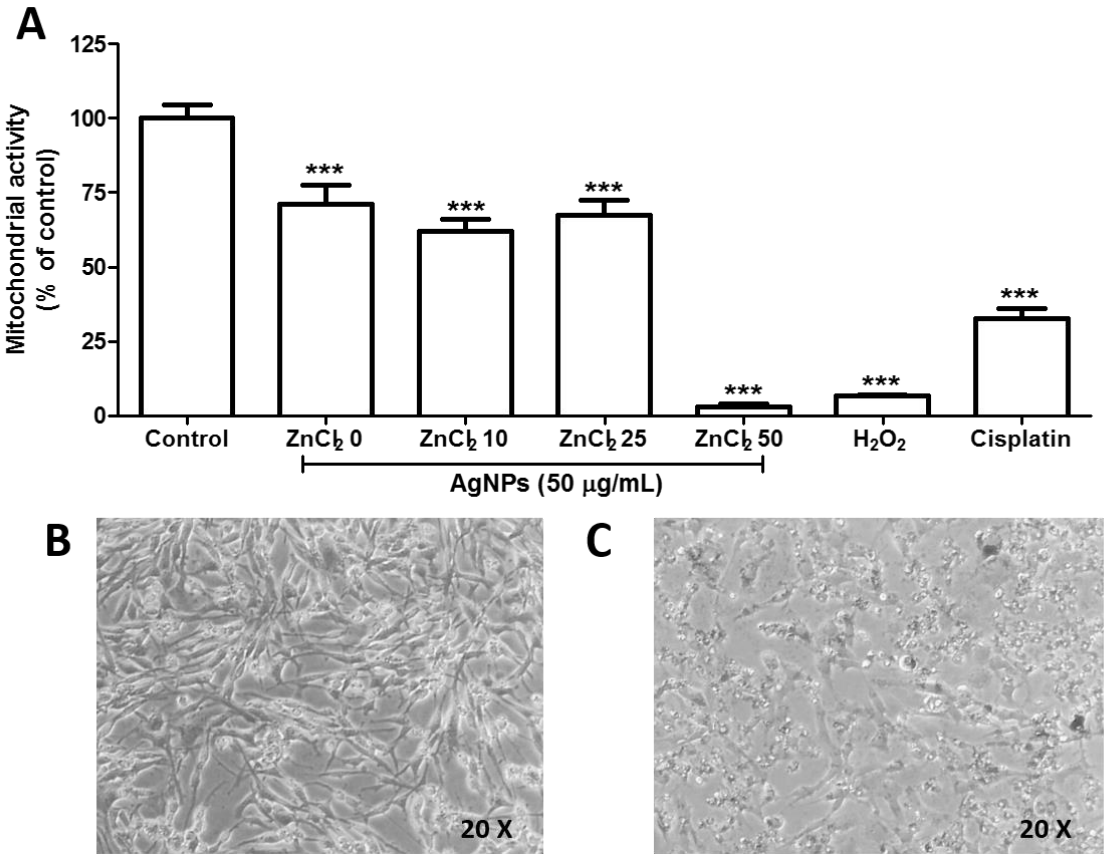
A
Mitochondrial activity (% of control)
125
100
75
50
25
0
***
***
***
***
***
***
Control
ZnCl2 0
ZnCl2 10
ZnCl2 25
ZnCl2 50
H2O2
Cisplatin
AgNPs (50 μg/mL)
B
20 X
C
20 X

Figure 5

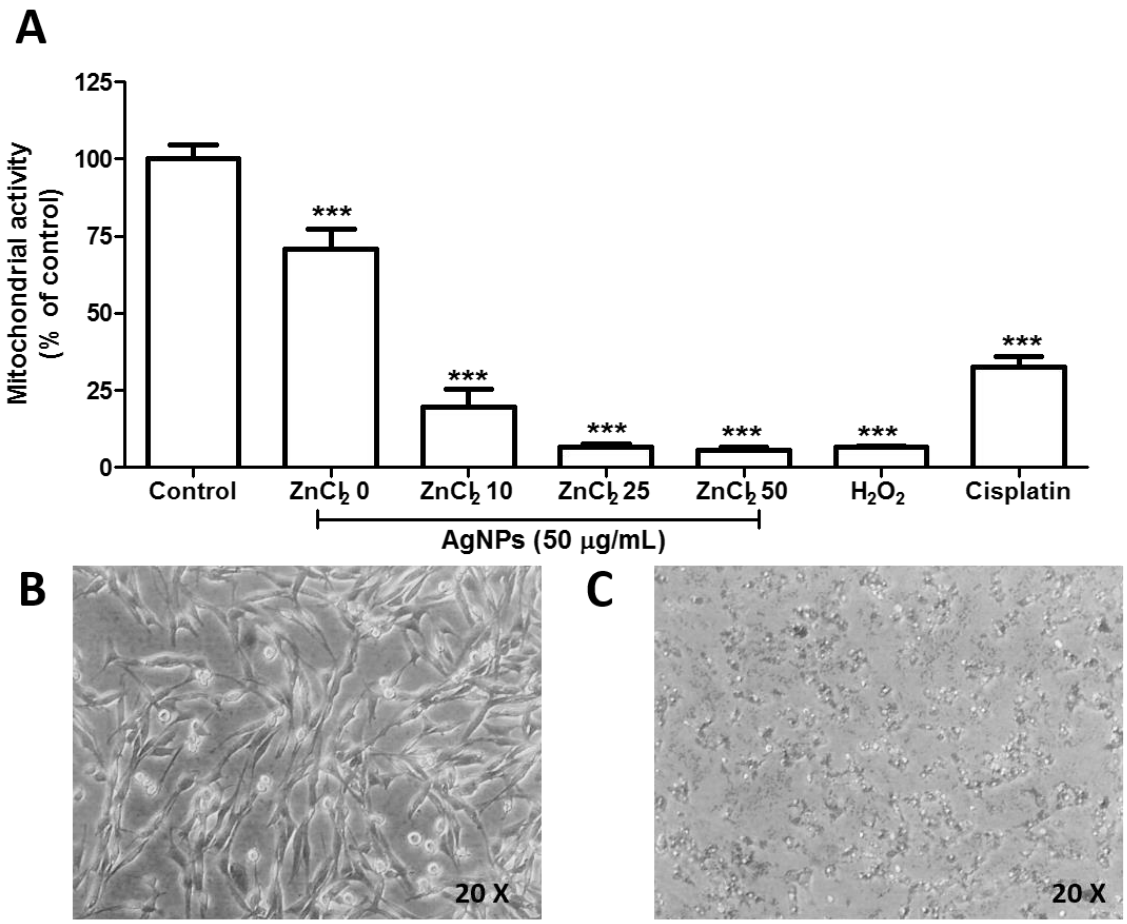
A
Mitochondrial activity (% of control)
125
100
75
50
25
0
***
***
***
***
***
***
Control
ZnCl2 0
ZnCl2 10
ZnCl2 25
ZnCl2 50
H2O2
Cisplatin
AgNPs (50 μg/mL)
B
20 X
C
20 X

Figure 6

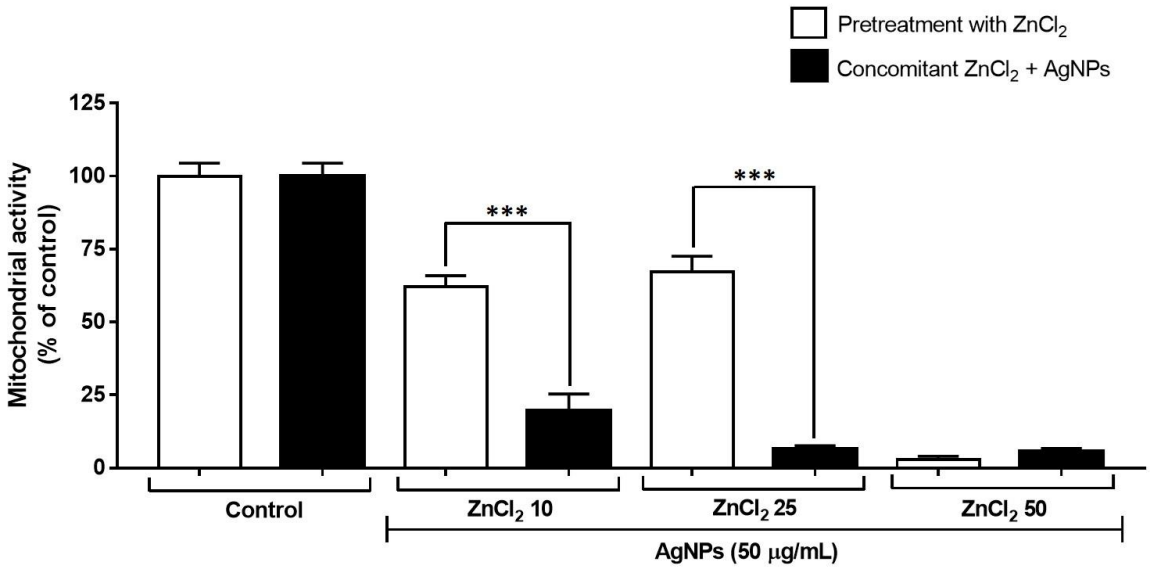
Pretreatment with $ZnCl_2$
Concomitant $ZnCl_2$ + AgNPs
Mitochondrial activity (% of control)
125
100
75
50
25
0
***
***
Control
$ZnCl_2$ 10
$ZnCl_2$ 25
$ZnCl_2$ 50
AgNPs (50 μg/mL)

Figure 7

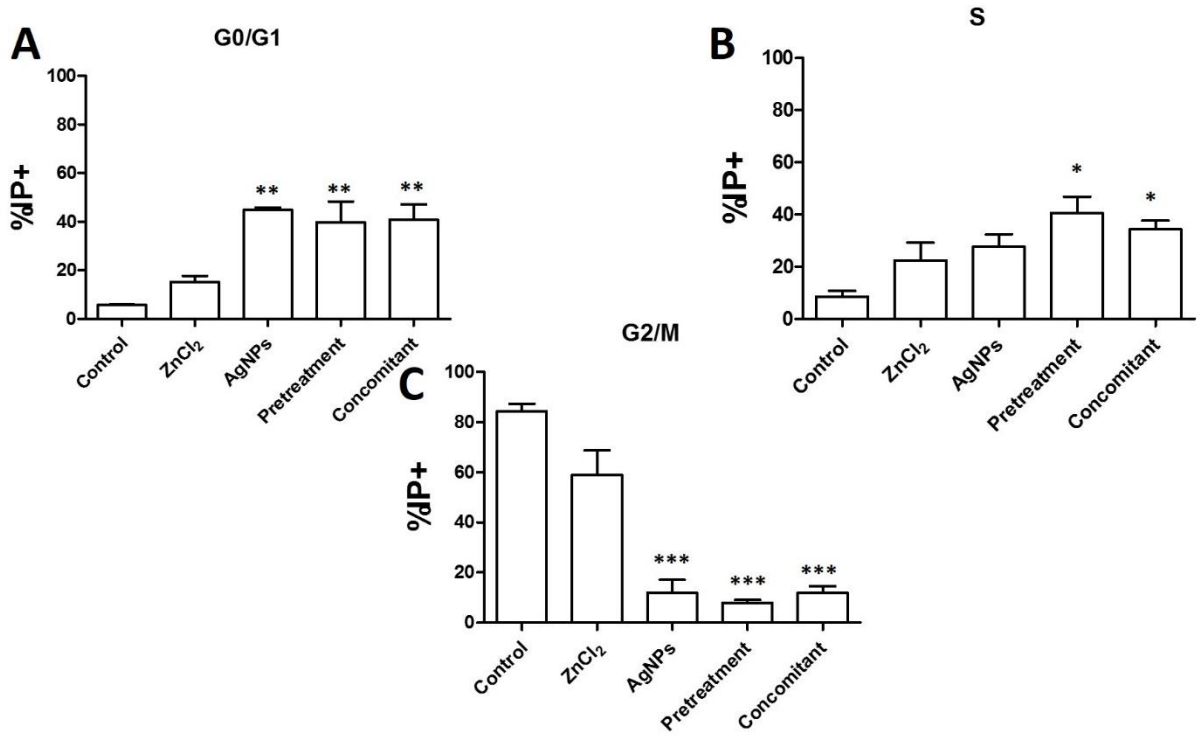
A
G0/G1
%IP+
100
80
60
40
20
0
**
**
**
Control
ZnCl2
AgNPs
Pretreatment
Concomitant
B
S
%IP+
*
*
C
G2/M
%IP+
***
***
***

Figure 8

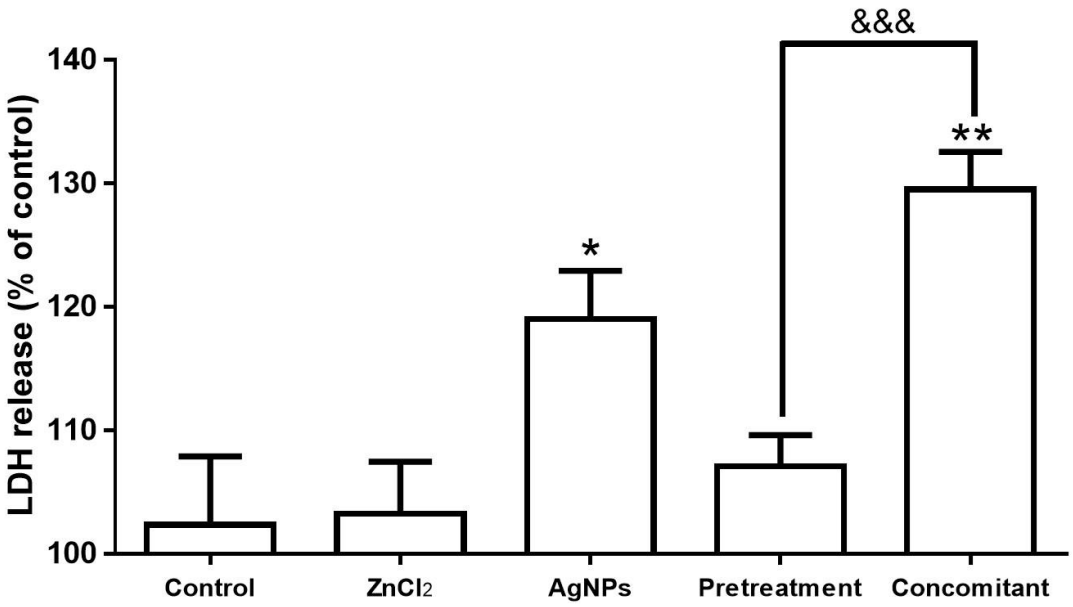
&&&
**
*
140
130
120
110
100
LDH release (% of control)
Control
ZnCl2
AgNPs
Pretreatment
Concomitant

9. References

AshaRani P V., Mun GLK, Hande MP, Valiyaveettil S (2009) Cytotoxicity and genotoxicity of silver nanoparticles in human cells. ACS Nano. doi: 10.1021/nn800596w

Beljanski M, Crochet S (1994) Differential effects of ferritin, calcium, zinc, and gallic acid on in vitro proliferation of human glioblastoma cells and normal astrocytes. J Lab Clin Med. doi: 10.1111/j.1365-2621.2010.02361.x

Bopp SK, Lettieri T (2008) Comparison of four different colorimetric and fluorometric cytotoxicity assays in a zebrafish liver cell line. BMC Pharmacol. doi: 10.1186/1471-2210-8-8

British Standards Institution (2007) Terminology for nanomaterials. Publicly Available Specif 16. doi: 9780580613210

Chen WQ, Cheng YY, Zhao XL, et al (2006) Effects of zinc on the induction of metallothionein isoforms in hippocampus in stress rats. In: Experimental Biology and Medicine

Denizot F, Lang R (1986) Rapid colorimetric assay for cell growth and survival. Modifications to the tetrazolium dye procedure giving improved sensitivity and reliability. J Immunol Methods. doi: 10.1016/0022-1759(86)90368-6

Doblas S, He T, Saunders D, et al (2010) Glioma morphology and tumor-induced vascular alterations revealed in seven rodent glioma models by in vivo magnetic resonance imaging and angiography. J Magn Reson Imaging. doi: 10.1002/jmri.22263

Espinosa-Cristobal LF, Martinez-Castañon GA, Loyola-Rodriguez JP, et al (2013) Toxicity, distribution, and accumulation of silver nanoparticles in Wistar rats. J Nanoparticle Res 15:. doi: 10.1007/s11051-013-1702-6

Franciscato C, Moraes-Silva L, Duarte FA, et al (2011) Delayed biochemical changes induced by mercury intoxication are prevented by zinc pre-exposure. Ecotoxicol Environ Saf 74:480–486. doi: 10.1016/j.ecoenv.2010.11.011

Fouad AS, Hafez RM (2018) The effects of silver ions and silver nanoparticles on cell division and expression of cdc2 gene in Allium cepa root tips. Biol Plant. doi: 10.1007/s10535-017-0751-6

Kim TH, Kim M, Park HS, et al (2012) Size-dependent cellular toxicity of silver nanoparticles. J Biomed Mater Res - Part A 100 A:1033–1043. doi: 10.1002/jbm.a.34053

Liu W, Worms IAM, Herlin-Boime N, et al (2017) Interaction of silver nanoparticles

with metallothionein and ceruloplasmin: Impact on metal substitution by Ag(i), corona formation and enzymatic activity. Nanoscale 9:6581–6594. doi: 10.1039/c7nr01075c

Luther EM, Schmidt MM, Diendorf J, et al (2012) Upregulation of metallothioneins after exposure of cultured primary astrocytes to silver nanoparticles. Neurochem Res 37:1639–1648. doi: 10.1007/s11064-012-0767-4

Mahmoudi M, Azadmanesh K, Shokrgozar MA, et al (2011) Effect of nanoparticles on the cell life cycle. Chem. Rev.

Maret W (2013) Zinc Biochemistry: From a Single Zinc Enzyme to a Key Element of Life. Adv Nutr. doi: 10.3945/an.112.003038

Moreno-Vilet L, Garcia-Hernandez MH, Delgado-Portales RE, et al (2014) In vitro assessment of agave fructans (Agave salmiana) as prebiotics and immune system activators. Int J Biol Macromol. doi: 10.1016/j.ijbiomac.2013.10.039

Perrin L, Roudeau S, Carmona A, et al (2017) Zinc and Copper Effects on Stability of Tubulin and Actin Networks in Dendrites and Spines of Hippocampal Neurons. ACS Chem Neurosci. doi: 10.1021/acschemneuro.6b00452

Prasad AS, Beck FWJ, Snell DC, Kucuk O (2009) Zinc in cancer prevention. Nutr. Cancer

Ruttkay-Nedecky B, Nejdl L, Gumulec J, et al (2013) The role of metallothionein in oxidative stress. Int J Mol Sci 14:6044–6066. doi: 10.3390/ijms14036044

Salazar-García S, Silva-Ramírez AS, Ramirez-Lee MA, et al (2015) Comparative effects on rat primary astrocytes and C6 rat glioma cells cultures after 24-h exposure to silver nanoparticles (AgNPs). J Nanoparticle Res 17:1–13. doi: 10.1007/s11051-015-3257-1

Silva-Ramirez AS, Castillo CG, Navarro-Tovar G, et al (2018) Bioactive Isomers of Conjugated Linoleic Acid Inhibit the Survival of Malignant Glioblastoma Cells But Not Primary Astrocytes. Eur J Lipid Sci Technol. doi: 10.1002/ejlt.201700454

Specification PA (2007) Terminology for nanomaterials. British Standards Institute, London 253 Page 12 of 13 J Nanopart Res (2020) 22:253

Sukhanova A, Bozrova S, Sokolov P, Berestovoy M, Karaulov A, Nabiev I (2018) Dependence of nanoparticle toxicity on their physical and chemical properties. Nanoscale Res Lett 13(1):44

Urbańska K, Pająk B, Orzechowski A, Sokołowska J, Grodzik M, Sawosz E, Szmidt M, Sysa P (2015) The effect of silver nanoparticles (AgNPs) on proliferation and apoptosis of in ovo cultured glioblastoma multiforme (GBM) cells. Nanoscale Res

Lett 10(1):98

Zhang T, Wang L, Chen Q, Chen C (2014) Cytotoxic potential of silver nanoparticles. Yonsei Med J 55(2):283–291 P